

# EFFECTS OF RF INTERFERENCE ON RADAR RECEIVERS

Frank H. Sanders,<sup>1</sup> Robert Sole,<sup>2</sup> Brent L. Bedford,<sup>1</sup> David Franc,<sup>3</sup> and Timothy Pawlowitz<sup>4</sup>

This report describes the results of interference tests and measurements that have been performed on radar receivers that have various missions in several spectrum bands. Radar target losses have been measured under controlled conditions in the presence of radio frequency (RF) interference. Radar types that have been examined include short range and long range air traffic control; weather surveillance; and maritime navigation and surface search. Radar receivers experience loss of desired targets when interference from high duty cycle (more than about 1-3%) communication-type signals is as low as -10 dB to -6 dB relative to radar receiver inherent noise levels. Conversely, radars perform robustly in the presence of low duty cycle (less than 1-3%) signals such as those emitted by other radars. Target losses at low levels are insidious because they do not cause overt indications such as strobes on displays. Therefore operators are usually unaware that they are losing targets due to low-level interference. Interference can cause the loss of targets at any range. Low interference thresholds for communication-type signals, insidious behavior of target losses, and potential loss of targets at any range all combine to make low-level interference to radar receivers a very serious problem.

Key words: radar interference; radar interference vulnerability; radar performance degradation; radar target loss; radar target detection; RF interference; UWB interference effects

## 1 RADAR FUNDAMENTALS RELATED TO INTERFERENCE TESTING AND MEASUREMENTS

### 1.1 Introduction

Radars play critical roles in national security, air traffic control, weather observation and warning, scientific applications, mapping, search and rescue operations, and other safety-of-life missions. Radar transmitter and receiver characteristics are engineered to successfully accomplish their missions in these areas. The technical characteristics of radars (such as high peak power levels emitted by the transmitters and very sensitive designs for the receivers) have usually resulted in exclusive, or at least primary, spectrum allocations for their operations.

In recent years, spectrum crowding has led to proposals for reduction of available spectrum for exclusive or primary radar operations, as well as for co-channel (or nearly co-channel) spectrum

---

<sup>1</sup> Institute for Telecommunication Sciences, National Telecommunications and Information Administration (NTIA), U.S. Department of Commerce, Boulder, CO.

<sup>2</sup> Office of Spectrum Management (OSM), NTIA, Washington, DC.

<sup>3</sup> National Oceanic and Atmospheric Administration (NOAA), formerly with the National Weather Service (NWS), Washington, DC.

<sup>4</sup> Federal Aviation Administration (FAA), Washington, DC.

sharing between radars and non-radar radio signals. It has been proposed in various forums, for example, that communication signals can (and should) sometimes share spectrum bands with radar systems. Such proposals typically presume that radar receivers will not suffer undue loss of technical performance due to such sharing so long as the interference levels are relatively low. Some sharing analyses assume that radar receivers are relatively robust against radio frequency (RF) interference effects from low levels of non-radar signals.

These proposals raise critical technical questions. These include: At what power levels do interfering signals cause adverse effects on the performance of these receivers? How are interference effects manifested in these radar receivers? Specifically, what are the interference levels at which radar receivers lose desired targets, and do low-level interference effects create observable manifestations on radar receiver displays?

NTIA, in cooperation with other US Government agencies and the United Kingdom (UK),<sup>5</sup> has performed a series of tests and measurements of the response of microwave radars to low levels of RF interference from a variety of communication and non-communication signals. This report describes the results of interference tests and measurements on several representative radar receivers. Interference data have been collected on radars performing various missions in several different spectrum bands. Radar types that have been examined include short range air traffic control; long range air traffic control; fixed weather surveillance; airborne weather surveillance; and maritime navigation and surface search. These radars have been operational in the spectrum bands 1200-1400 MHz; 2700-2900 MHz; 2900-3700 MHz; and 8500-10500 MHz.

## **1.2 Noise Versus Interference**

Radars operate by directing transmitted radio energy through space toward remote objects that need to be observed and subsequently receiving and processing reflections of small portions of the transmitted energy returned as echoes from the desired objects (called targets). The time delay between transmission and reception of the energy is used to determine the distances between the radar and the targets, while the direction in which the energy is initially directed and then returned as reflections informs the direction of the targets from the radar. Ultimately, the key to successful radar design is the solution of two technical problems: generation and direction of an adequate amount of radio energy from the transmitter in sufficiently localized directions through space; and the reception, detection, and discrimination of the small fraction of energy that has been reflected from both desired targets and undesired reflecting objects (collectively called clutter) in the presence of natural (and sometimes manmade) noise in the radar receiver.

This report addresses the general question of how, and to what extent, RF interference causes degradation to the performance of radar receivers. Before interference effects are discussed, it is necessary to define interference, describe how it differs from other environmental degradation effects, and explain why it is considered separately from those effects. It is also necessary to describe the normal processes of target reception, detection, and discrimination in radar receivers. Those topics are addressed in the following parts of this report section.

---

<sup>5</sup> Including the National Oceanic and Atmospheric Administration (NOAA), U.S. Coast Guard (USCG), Federal Aviation Administration (FAA), and the United Kingdom's (UK) Fraser Test Range at Portsmouth.

### 1.2.1 Definition and Distinction of Noise Versus Interference

Unwanted energy coupled into radar receivers from natural sources and from manmade devices that are not intentional radio transmitters is called *noise*. Noise degrades radar receiver performance and is generated by many sources. A natural source is the energy produced by thermal electrons within radar receiver circuitry; it is one of the most fundamental limiting factors in radar receiver performance. Other noise is coupled into radar receivers from naturally occurring, distant sources. In the high frequency (HF) spectrum these prominently include noise from lightning strokes reflected from our planet's ionosphere and (as a smaller effect) Jupiter, while at higher frequencies (very high frequency (VHF), ultrahigh frequency (UHF), and lower microwave), important noise sources are the Sun and to a lesser extent our galactic center and a variety of other astronomical objects. Manmade noise across the spectrum from HF to lower microwave frequencies (around 1.5 GHz) is coupled into radar receivers from unintentional emission sources such as electric motors, above-ground power lines, and automotive ignition systems. Spectrum survey data [1-4] indicate that manmade noise levels tend to decrease below receiver thermal noise at higher microwave frequencies (above about 1.5 GHz), although some sources (e.g., microwave ovens) can produce significant background microwave emissions in industrial, scientific, and medical (ISM) radio bands such as at 2.5 GHz [5-8].

Randomly distributed radio energy from all sources, both natural and manmade, combines to generate overall environmental background noise against which radar receivers must always perform. Noise sources are unavoidable and generally uncontrollable. However, they do produce known background levels, their emissions obey well-understood patterns in time and space, and they are generally predictable in both their location and their timing (e.g., the diurnal location and movement of astronomical sources across the celestial sphere and the diurnal power levels, cycles, and spectrum ranges of manmade noise near cities, highways, and industrial zones).

In contrast to noise, *interference* is unwanted radio energy<sup>6</sup> coupled into radar receivers from manmade, intentional radio transmitter sources such as communication devices. Like noise, interference degrades radar receiver performance. Interference, however, generally has statistical and spectrum characteristics that are different from noise. Another important contrast between noise and interference is that, while noise may be unavoidable and largely uncontrollable, interference is both avoidable and controllable through sound spectrum engineering and management procedures.

Although both noise and interference cause degradation in radar receiver performance, the existence of noise does not logically imply that radar receivers should therefore be expected to operate in the presence of interference. If any connection is to be drawn between the two phenomena, it is that the existence of noise as a source of uncontrollable and unavoidable degradation in radar environments implies that interference (which in contrast, and by definition, is both controllable and avoidable) must be restricted all the more carefully in order not to add to the inevitable performance degradation caused by environmental noise.

Noise phenomena and their effects on radar receiver performance have been treated extensively in existing technical literature [9-12, for example]. Noise effects are typically taken into account

---

<sup>6</sup> Interference is sometimes defined as the *effect* of unwanted energy in a receiver, rather than the energy itself.

in radar receiver design and are distinct and separable in both their origins and their behavior from interference effects. For these reasons, and because interference is a controllable phenomenon, this report does not address noise effects in radar receivers other than as an inherent limiting factor generated by thermal electron activity in receiver circuitry. Only interference degradation effects on radar receivers are addressed in this report.

### 1.3 Detection of Radar Targets

Radar targets are detected by transmitting radio energy into space, receiving a portion of the transmitted energy that is reflected as echoes from targets, and processing it inside receiver circuitry to separate the echo energy from whatever noise and interference are present in the receiver. A radar will always have a maximum range that is a function of the transmitter power, the degree to which the transmitted energy is confined directionally in space, the effective area of the receiving antenna, the efficiency with which targets reflect radio energy at the radar frequency, and the minimum threshold within the receiver for detection of echo energy.

#### 1.3.1 The Radar Equation

Assuming theoretically perfect free-space radio signal propagation conditions, the maximum range of a radar,  $R_{max}$ , is given by the so-called radar equation (modified from [9, pg. 15]):

$$R_{max} = \left[ \frac{P_t G_t A_e \sigma_0}{(4\pi)^2 L_s S_{min}} \right]^{1/4} \quad (1)$$

where:

$P_t$  = transmitted power, watts;

$G_t$  = gain of the transmitter antenna, linear term;

$A_e$  = effective aperture of the receiving antenna,  $m^2$ ;

$\sigma_0$  = nominal (specified) target cross section,  $m^2$ ;

$L_s$  = system loss between transmitter/receiver and antenna, linear dimensionless quantity;

$S_{min}$  = minimum detectable signal, watts.

With the exception of the target cross section term,  $\sigma_0$ , all of the variables in (Eq. 1) are in principle controllable by radar designers (although there are practical limits on all of the variables).  $R_{max}$  is a theoretical maximum that is never realized due to practical engineering and design limitations of field-deployed equipment and unanticipated losses within radar systems. Actual values of  $R_{max}$  are typically half of the theoretical value [9]. A variety of environmental factors tend to decrease radar range. These include propagation losses that exceed the free-space assumption of the radar equation as well as fluctuations in the radar cross sections of targets.

### 1.3.2 Radar Target Detection Probability

The peak values of transmitted power,  $P_t$ , that are required for effective observation and tracking of radar targets are so high that they often can only be generated for short intervals. Furthermore, most radar designs require that the radar transmitters be periodically turned off so that the receivers can listen for the target echoes. Therefore most radars transmit radio energy in pulses.<sup>7</sup>

Detection of radar targets is a probabilistic process; for any given target, there is a probability that it will be detected as an echo from any individual pulse of transmitted energy. But the probability of detection on a per-pulse basis is usually too low for effective radar operations. The per-pulse detection probability can be increased by raising the values of the parameters in (Eq. 1), but in well-engineered radars the values of the (Eq. 1) parameters have already reached the limits of available technology and practicality. The only way to obtain high probabilities of target detection is to illuminate a target with more than one pulse, so that the cumulative probability of detection becomes adequate for effective operations. In the most simplistic approach, it is established that the probability of detection per pulse is  $x$  (where  $x < 1$ ). The probability of not detecting a target with a single pulse is thus  $(1-x)$ . Assuming independence of detection probability from pulse to pulse, the probability of *not* detecting a target with any of  $n$  pulses is  $(1-x)^n$ . The probability of detection of a target,  $P_d$ , with at least one of  $n$  pulses is unity minus that value:

$$P_d(x, n) = 1 - (1 - x)^n. \quad (2)$$

Figure 1 illustrates the principle of variation of  $P_d$  as a function of  $n$  for a variety of values of  $x$ . For typical operational radar designs,  $n$  is often between 10 and 20. When fewer than 10 pulses illuminate a target, detection probability is low and detection probability increases rapidly with the use of additional pulses. But detection probability only increases slowly after more than about 20 pulses are used on a target; diminishing returns in radar performance relative to longer dwell times on each target tend to preclude the use of many more pulses for illumination.<sup>8</sup> The need for targets to be illuminated with 10 to 20 pulses leads in turn to the selection of a variety of additional radar parameter values, such as the maximum rate that the radar beam may be scanned through space.<sup>9</sup>

Explained another way, the low per-pulse probability of detection must be somehow overcome to make radars work effectively. Since the parameters in (Eq. 1) (such as transmitter power and antenna gain) have already been optimized in good radar designs, the only remaining method for reliably observing targets is through receiver processing of multiple pulses reflected from each target. This is receiver processing gain. Although processing gain enhances target detection, and may tend to mitigate some special types of interference (such as from pulsed sources that

---

<sup>7</sup> Some radars, especially those used for certain types of target tracking, do transmit continuously.

<sup>8</sup> There are some exceptions. For example, some meteorological radars examine the very weakly reflecting phenomena of high-altitude winds. These radars, called wind profilers, may need to integrate echo energy from tens of thousands of pulses over a period of a few minutes in order to generate a single data point.

<sup>9</sup> For example, if a radar must have a 200 nm range and at least 15 pulses must illuminate each target within a 1-degree wide beamwidth, then the radar must scan at a rate that is not faster than one revolution every 13.4 sec. This of course becomes the lower bound for the time interval between updates on target locations.

transmit energy at a low (less than 1 per cent) duty cycle), it is not an interference rejection technique per se.

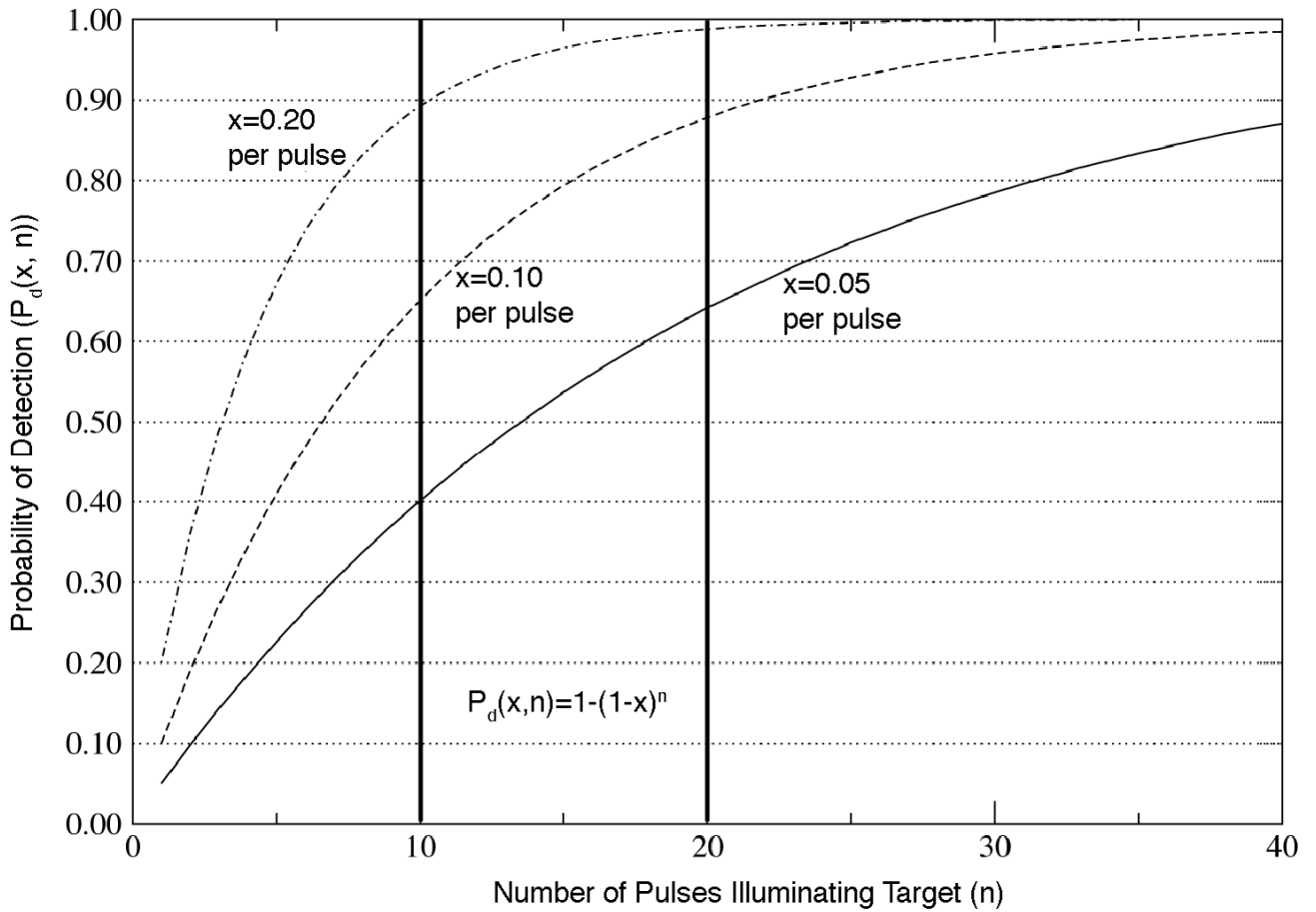


Figure 1. Probability of detection versus number of radar pulses illuminating a target for three probabilities per pulse, from (Eq. 2):  $x=0.05$ ,  $x=0.10$ , and  $x=0.20$ . Many radars balance the need to detect targets with high probability against the need to update scans in a timely manner by using between 10 to 20 pulses per target (indicated with solid vertical lines).

#### 1.4 Radar Receiver Inherent Noise

As noted in Section 1.2, one of the most fundamental limitations on microwave radar receiver performance is inherent, internal noise generated by thermal electrons in receiver circuitry. The average power level in watts,  $P$ , of this noise is:

$$P = kTB \quad (3)$$

where:

$k$  = Boltzmann's constant ( $1.38 \cdot 10^{-23}$  J/(K·Hz));  
 $T$  = temperature of the circuitry (K);  
 $B$  = bandwidth of the circuitry (Hz).

For example, a circuit at room temperature (about 290 K) operating in a bandwidth of 1 MHz ( $10^6$  Hz), will have an inherent noise level of  $4 \cdot 10^{-15}$  W, or -144 dBW, or -114 dBm.

The *noise factor*,  $f_n$ , of a receiver is defined as:

$$f_n = \frac{N_{out}}{kTB} = \left( 1 + \frac{\Delta N}{kTB} \right) \quad (4)$$

where:

$N_{out}$  = total available output noise power from the circuit;  
 $\Delta N$  = noise power in addition to  $kTB$  generated by the circuit.

The *noise figure*,  $F_n$ , of the circuit, a decibel quantity, is defined as:

$$F_n = 10 \log(f_n). \quad (5)$$

Ideally,  $N_{out} = kTB$ , or, equivalently,  $\Delta N = 0$ . If this performance could be achieved, then the noise factor of the receiver would be unity and the noise figure of the receiver would be zero decibels. The sensitivity of such a receiver would be theoretically optimal.

Realistically, such performance is impossible; the values of  $N_{out}$  and  $\Delta N$  will be somewhat larger than  $kTB$  and zero, respectively. In a well-designed receiver in which the noise figure and gain characteristics of the first low-noise amplifier (LNA) are properly cascaded with all of the circuitry after the LNA, the LNA noise figure will nearly determine the overall noise figure of the entire receiver. A high-performance LNA noise figure in a radar receiver is a few decibels higher than  $kTB$ . Insertion loss of components in the radar receiver ahead of the LNA (such as RF band-limiting filtering) will add directly to the overall noise figure of the receiver. Such losses can add up to another decibel or more.

In practice, an overall noise figure of 10 dB is an easily achievable value for radar receivers, while a value of 5 dB or less is usually considered to be nominal. To continue with the example given above, if  $kTB$  is -114 dBm and the noise figure of the receiver is 5 dB, then the radar receiver overall noise level will be effectively -109 dBm. Ultimately, all desired targets must somehow be detected against receiver noise.

## 1.5 Minimum Detectable Signal

Figure 1 illustrates the importance of obtaining the highest possible probability of detection on a per-pulse basis for the overall problem of detecting targets with  $n$  pulses. Each pulse is detected relative to radar receiver noise. The total signal power available to the receiver from all pulse echoes is  $S$ . There is a minimum  $S$  value,  $S_{min}$  (Eq. 1), which determines the maximum radar range,  $R_{max}$ , for a given target cross section. (It can also be used to determine the minimum target cross section that may be detected at any range.) This critical ( $S_{min}$ ) itself is limited by the radar receiver inherent noise.

If a radar is barely able to detect a target at maximum range,  $R_{max}$ , then the corresponding minimum signal-to-noise ratio,  $(S/N)_{min}$ , must be related to  $S_{min}$  as follows:

$$S_{min} = kTBF_n \left( \frac{S}{N} \right)_{min} . \quad (6)$$

For a false-alarm probability of  $10^{-6}$ , a detection probability of 0.8, and a standard echo-power variation model (Swerling case 1, see Section 1.7 below), the required signal-to-noise ratio is about 17 dB [12, pg. 24], which is a linear factor of 50:1. With a nominal noise figure of 5 dB (a linear factor of 3.16), the value of (Eq. 6) in a (nominal) 1-MHz bandwidth is  $S_{min}=6.3 \cdot 10^{-13}$  W.

The value of  $S_{min}$  is further reduced by the effect of integrating  $n$  pulses, where typically  $n=20$ . This effect results in a value of  $S_{min}$  that is about  $10^{-13}$  W [12, pg. 25].

Although (Eq. 6) is obtained by inverting (Eq. 1) for the maximum detection range of a target with a nominal cross section  $\sigma_0$ , it is important to note that the value of  $S_{min}$  of  $10^{-13}$  W is itself independent of range. Any target, at any range, that returns less than this much energy to the radar receiver will probably not be observed on a radar display. If all targets had the nominal cross section  $\sigma_0$  of (Eq. 1), then  $S_{min}$  would be returned only by targets at the edge of the coverage range and all targets within that range would be detected. But in reality, cross sections vary widely and many targets will have cross sections that are less than  $\sigma_0$ . Such targets will be lost at distances less than  $R_{max}$ .

## 1.6 Increase in Receiver Noise Figure as a Function of Interference Power Level

If interference is introduced into a radar receiver, the average power contribution from the interference,  $I$ , will sum with the radar inherent noise power,  $N$ , and that summed power will tend to mask the detection of desired targets. The ratio of the summed noise-plus-interference to inherent noise is  $(I+N)/N$ , and its behavior relative to the ratio of  $I/N$  is portrayed graphically in Figure 2.

As shown in Figure 2, the receiver noise figure is increased by 0.5 dB when the average interference power is 9.5 dB below the nominal receiver noise level, and the receiver noise figure is increased by 1 dB when the average interference power is 6 dB below the nominal receiver noise level. *These effective noise figure increases would represent equal increases in the minimum detectable signal level of radar receivers that are subjected to interference.*



## 1.7 Detection of Radar Targets When Their Levels Fluctuate

The power level of echoes from radar targets will normally vary in time. Such variations may occur due to time-dependent changes in the range, the aspect angle of the target, and the propagation and multi-path characteristics between the radar and the target. The result is that the variable of cross section in (Eq. 1),  $\sigma_0$ , is really a time-varying effective cross section,  $\sigma_{eff}(t)$ .

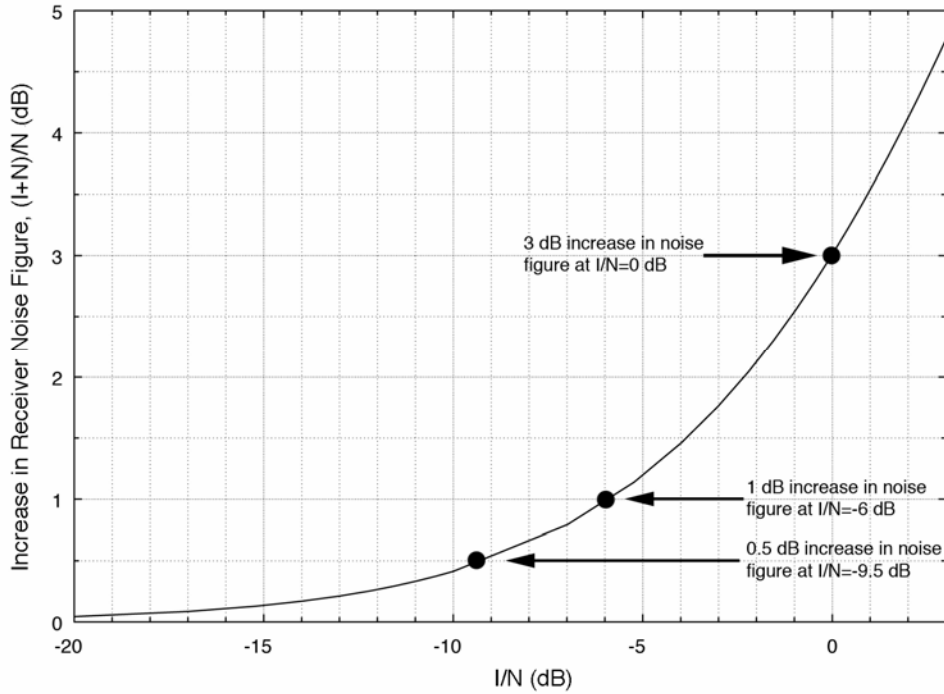


Figure 2. Receiver noise figure increases as the sum of interference power,  $I$ , and inherent internal noise,  $N$ , divided by the same noise power:  $(I+N)/N$ . This is the relation between  $(I+N)/N$  and  $I/N$ .

How do radar designers take these fluctuations in effective target cross sections into account when they design the systems? A naïve approach would be to increase radar transmitter power to accommodate the deeper power dips in such fluctuations. But this is not practical because the capacity for high peak power generation in radar transmitters is very expensive. Furthermore, most radar transmitters are designed to produce the highest possible peak power levels that technology can create and that budgets can afford. Thus it is not generally possible to increase the transmitter peak power, and another way must be found to compensate for target power fluctuations.

The compensation method that is actually implemented is to transmit *more pulses* at fluctuating targets than would have been needed if the targets had constant echo amplitudes, and to integrate the resulting multiple echoes to detect targets even when they are weaker than the nominal cross section. The approach is explained in standard radar design references [9-15, for example]. In this approach, standard mathematical models are used to describe the statistical characteristics of radar echo amplitudes. But however useful such models are when applied to radar design, they

ironically do not reproduce the behavior of real radar targets [9, pg. 52]. “The uncertainty regarding fluctuating target models makes the use of the constant (non-fluctuating) cross section in the radar equation an attractive alternative when a priori information about the target is minimal,” [9, pg. 52].

## 1.8 Criteria for Radar Receiver Interference Thresholds

A recent, comprehensive compilation of currently accepted interference criteria from the existing literature indicates that currently accepted limits on  $I/N$  for carrier wave (CW) and noise-like interference in radar receivers are currently between -6 dB to -10 dB [16, pp. 5-2 and 5-3]. No standards currently exist for any other categories of interference (e.g., digital signal modulations) in radar receivers.

Based on the existing literature on this subject [16], limits on  $I/N$  in radar receivers are understood to mean the maximum allowable ratio of interference power to radar receiver noise power in the IF stages of radar receivers. The protection criteria that have been identified *do not* ensure that interference effects will not occur at (or below) those  $I/N$  levels; rather, it has simply been generally understood that these values should not be exceeded unless additional compatibility studies are performed which show that higher  $I/N$  levels would be acceptable under any given set of circumstances for any given type of radar receiver. The state of the existing literature on this subject begs several questions:

- 1) Is a limit on the  $I/N$  ratio in a radar receiver IF stage necessarily the best (or most appropriate) criterion for interference protection?
- 2) How reliable is the range of existing  $I/N$  protection criteria of -6 dB to -10 dB for protection of radar receivers from CW and noise-like interference?
- 3) For types of interference other than CW and noise-like (e.g., digital signal modulations), what should be the  $I/N$  protection criteria for radar receivers?
- 4) Can tighter bounds be placed on interference protection criteria for radar receivers?

In answer to the first question, alternative proposals have been variously problematic because they do not address some types of radar, or because they invoke protection criteria that cannot be analyzed or verified in any practical sense for operational, deployed systems. For example, it has been proposed that interference might be allowed to occur in some types of radar receiver in some spectrum bands on a statistical basis, with more interference allowed for shorter amounts of time and lower interference allowed for longer periods, according to some sort of predetermined ‘interference budget.’ But one of the problems with this approach is that no practical method has been identified for monitoring such interference in radar receivers, determining the sources, computing the current state of the interference budget from the interfering sources, and then somehow communicating from the radars to the interference sources that those sources must modify (in some unspecified way) their operations so as to mitigate the interference they are generating. In contrast, the approach of analyzing worst-case interference levels in radar receiver IF stages from the known characteristics of the radars and potential interference sources, while conservative, is nevertheless practical and verifiable (both theoretically and through

measurements), while providing assurance that critical radar missions (including safety-of-life) are not adversely impacted by interference sources. As documented in this report, degradation of radar receiver performance can be closely correlated with  $I/N$  levels in radar receivers for high-duty-cycle interference such as CW, noise, and digital signal modulations.

As for the remaining questions above, until now very little information has been available in the technical literature regarding the effects of low-level interference in radar receivers. It has therefore been debatable as to whether  $I/N$  interference protection limits of -6 dB to -10 dB  $I/N$  are necessarily appropriate for radar receivers in general, and whether those bounds might be determined more closely for various types of radar systems. These questions have been the impetus for the tests and measurements that are documented in this report.

## 1.9 Radar Detector Characteristics

The detector in a radar receiver is the device that extracts modulation information from the received carrier signal of the target echoes. The “detector” usually comprises the parts of the radar receiver between the output of the last IF amplifier and the input of the data processor (or other data display indicator). Detectors operate on both signal and noise inputs. The most widely used types are described below.

### 1.9.1 Envelope (Square-Law, Optimum-Law, or Quadratic) Detectors<sup>10</sup>

An envelope detector produces an output that is a function of the amplitude of the input waveform modulation envelope; phase information in the waveform is lost. The output of the detector is usually either a linear function of the input envelope<sup>11</sup> or, more commonly, is proportional to the square of the input envelope level. The response of an associated radar video integrator, if any exists, is normally included as part of the detector response for purposes of analysis. Empirical work [15, pp. 58-62] revealed that the optimum response function for a radar detector (when the signal-to-noise ratio of targets is small) is:

$$\psi(v) = Av^2 = y \quad (7)$$

where:

- $\psi$  = the output of the detector;
- $v$  = the amplitude of the modulation envelope of the input;
- $A$  = a scaling constant, often 1/2;
- $Y$  = the value of a single, discrete output from the detector.

The scaling constant,  $A$ , is only a multiplier of a bias level; it does not ultimately affect the  $P_d$  for a radar target. The square-law detector output usually feeds a linear-law video integrator. The integrator accumulates the results of  $n$  samples (such as from  $n$  pulses) [15, pg. 58]:

<sup>10</sup> The terms square-law, optimum-law, and quadratic detector are all used interchangeably.

<sup>11</sup> Noting that even so-called linear detectors are non-linear devices, by definition of detectors.

$$Y = \sum_{i=1}^n y_i = A \sum_{i=1}^n v_i^2 \quad (8)$$

where:

$Y$  = the output of the integrator;

$y_i$  = the amplitude of the  $i$ -th sample from the square-law part of the detector, from (Eq. 7).

The square-law detector-integrator is a simple and widely used device in radar receiver designs; as a default it is usually assumed to be the type of detector that is used in radar receivers. Linear-law detectors are not unknown, but their performance is generally similar to square-law detectors [15, pg. 62].

### 1.9.2 Logarithmic Amplifier Detectors

Some types of radar, such as maritime navigation units, experience a very wide range of echo amplitudes. This wide dynamic range of target echoes may span orders of magnitude, and will tend to exceed the response range of a single, linear receiver IF amplifier. To cope with this problem, *logarithmic amplifier* detectors are used. In logarithmic amplifier detectors, a cascaded chain of amplifier stages operates in parallel with a chain of envelope detectors to generate a receiver output that is proportional to the logarithm of the input envelope. Each stage in the cascade must have fixed, identical gain. A conceptual block diagram of a logarithmic amplifier detector is shown in Figure 3.

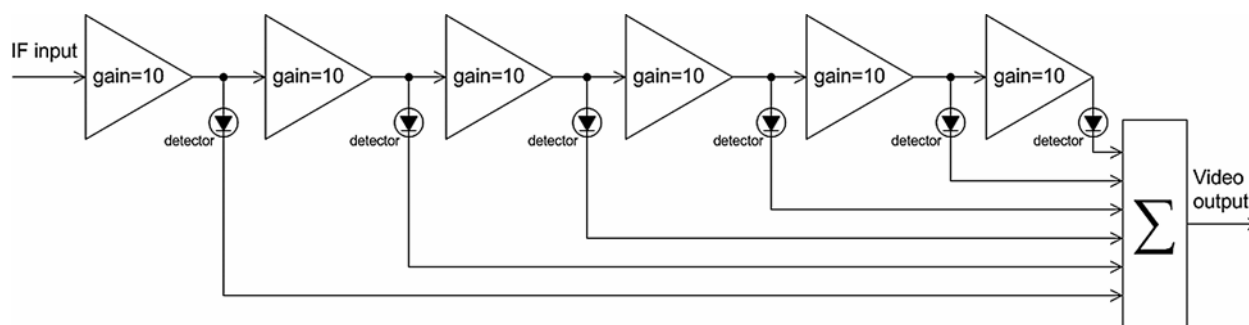


Figure 3. Block diagram of a logarithmic amplifier detector. The gain value of 10 is for example only.

The key principle of the design is that each detector is able to operate on the output of a graduating accumulation of gain. Thus the first detector operates on a small amount of gain that is suitable for very strong target echoes. Conversely, the last detector operates on perhaps 60 dB of gain, which will have been totally saturated for strong echoes but which is still adequate to provide a linear response to extremely weak target echoes. Thus strong target echoes produce outputs from all detector stages, extremely weak echoes produce an output from only the last detector stage, and all other echoes produce intermediate numbers of detector responses. The fact that the detector responses are finally summed means that a logarithmically varying range of output levels occurs across a very wide dynamic range of target inputs. Along with avoiding

saturation problems, logarithmic detectors also reduce the effects of unwanted clutter targets in radar receivers that do not have moving target indicator (MTI, or Doppler) processing (see below).

Logarithmic detectors cause a penalty in the probability of target detection that is manifested as a receiver gain reduction factor [9]. The reduction in the  $P_d$  as a function of the number of integrated pulse-echoes can be characterized as follows [9]: For 10 pulses integrated, logarithmic receiver loss is about 0.5 dB; for 100 pulses integrated, the loss is about 1.0 dB; and for an indefinitely large number of pulses integrated, effective reduction due to the use of a logarithmic detector maximizes at about 1.1 dB.

### **1.9.3 Zero-Crossings Detectors**

Zero-crossings detectors work on the principle that signals can be identified in noise by extracting information about the zero-crossings of the desired energy. The operative principle is that the average number of zero-crossings will decrease as signal-to-noise ratio increases. Put another way, the principle is that signal-plus-noise voltage will tend to exceed the voltage of noise alone. In a zero-crossings detector, a device is constructed that counts the average number of zero-crossings per unit time,  $n_{ave}$ , compares  $n_{ave}$  to a predetermined threshold value,  $T$ , and then declares that a target is present if ( $n_{ave} < T$ ). Whereas envelope detectors discard phase information in target echoes, zero-crossings detectors eliminate amplitude information about target echoes.

### **1.9.4 Coherent Detectors**

A coherent detector is a balanced mixer with a low-pass filtered output. One of the balanced mixer inputs is a reference signal, generated by an internal reference oscillator, which provides a signal with some specified frequency and phase. The other input of the mixer is from the last radar receiver IF amplifier. The detector works on the assumption that the frequency and phase of the target echo from the IF amplifier output matches the reference signal. The low-pass output filter allows only the dc and low-frequency modulation components to pass, rejecting higher frequencies near the carrier. In effect, the carrier frequency is translated to direct current.

Coherent detectors preserve both amplitude and phase information in target echoes, and are theoretically more efficient than envelope detectors (by about 1-3 dB), especially at low signal-to-noise ratios [9]. Coherent detectors are seldom used in radar receivers, however, because the phase of the received signal usually cannot be known or controlled relative to the phase of the transmitted pulse.

### **1.9.5 Moving Target Indicator (MTI) or Doppler Processing**

In many radar applications it is desirable and even necessary to distinguish moving targets from all other echo returns. This feature, called moving target indicator (MTI) or Doppler return processing, is ubiquitously implemented in air search radars. Although MTI processing is not

strictly a type of detection, its close integration with radar detection functions makes it worthwhile to mention in this context.

MTI works on the principle that electromagnetic echo energy emitted by a target that is moving with respect to the receiver platform will experience a Doppler shift in wavelength (and, consequently, frequency) compared to the wavelength of the radiation emitted by the radar transmitter. If echo energy is blocked in the receiver if it has the same frequency as the transmitted pulses, but is passed through the receiver otherwise, then only targets that are moving relative to the receiver will be displayed.

One low-cost method for implementing MTI is to lock a coherent oscillator (COHO) to the frequency of a set of individual transmitted pulses, use the COHO to beat against frequency of the echo returns from the same pulses, and filter the output with a DC block. This allows only non-zero beat frequency outputs to pass through the filter and be displayed. More costly MTI implementations may rely on high-precision frequency references for the generation of transmitted pulses.

Although MTI processing offers a number of advantages in terms of target discrimination, especially against clutter, it also has drawbacks. Some radars cannot use it because their PPI displays must show non-moving targets (e.g., floating debris and shorelines). Because MTI processing will be impaired by targets that are moving at speeds that cause the Doppler shift of the return echoes to be an integral multiple of the prf of the radar (e.g., a Doppler shift of 1 kHz or 2 kHz or 3 kHz, etc., in a radar that is transmitting a 1-kHz prf), radars that are designed for MTI must normally stagger the intervals between transmitted pulses by intervals that do not divide evenly into one another. Typically three or more such intervals must be generated between successive pulses to eliminate these so-called “blind speeds.” Staggering the transmitted pulses, providing for a precision frequency reference and/or COHO-mixer hardware in the transmitter, and incorporating MTI filters and software into the receiver adds to the cost and complexity of a radar. Furthermore, like all target-return processing, implementation of MTI will cause an effective increase in noise figure and the consequent loss of some desired targets from the PPI display under various circumstances. MTI processing does not reject interference.

### **1.10 Radar Features for Detection of Targets in Clutter and Interference**

Unwanted radar echoes are called clutter [9, pg. 470] because the output of the undesired echoes tends to clutter the radar display. Sources of clutter include terrain features and structures, ocean-surface features, precipitation, flocks of birds, and insect swarms. Small pieces of metal foil (chaff) intentionally ejected in the atmosphere cause degradation of radar performance by intentionally creating clutter effects. Regardless of the origin, clutter always tends to degrade radar performance. An example of clutter is shown in Figure 4.

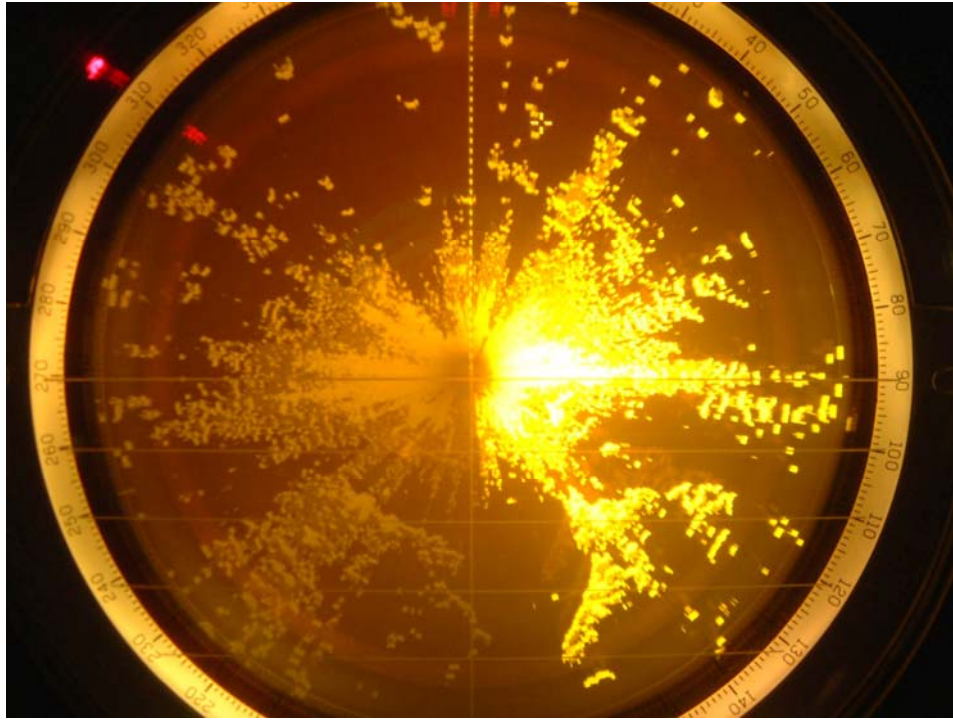


Figure 4. An example of clutter on a 9-GHz maritime radionavigation radar plan position indicator (PPI) display. The clutter includes local buildings, terrain, and vegetation. No intentional interference or test targets are present on this display.

Clutter effects may be mitigated by some radar design features. Since clutter sources tend to be either stationary or slow-moving, they may be somewhat reduced by the use of Doppler filtering (MTI) that eliminates the effects of echo energy with less than a minimum amount of frequency-shift relative to the transmitted frequency. However, motion characteristics of birds and insects do not always allow their echoes to be eliminated by such processing.

If fixed, ground-based clutter due to terrain is severe in the vicinity of a fixed-sited radar (an example being large hills or mountain ranges that protrude into the radar beam coverage), a clutter fence that is electromagnetically opaque may be built around part of the radar site. The fence attenuation may reduce the clutter effects, but will tend to adversely affect the radar performance in other respects [9, pg. 498].

Otherwise, clutter effects may be reduced generally by the use of the feature of sensitivity time control, as described below. None of the techniques that reduce clutter will mitigate the effects of radio interference in radar receivers.

### 1.10.1 Sensitivity Time Control (STC), or Swept Gain

*Sensitivity time control* (STC) suppresses the effects of clutter-producing objects that are located near the radar. STC reduces the dynamic range requirements of radar receivers by reducing receiver gain just after each pulse is transmitted. This sensitivity reduction, also called *swept gain*, is gradually recovered in a controlled manner, often as a fourth-power function of time [12,

pg. 13]. The receiver gain, in other words, is reduced for echoes that originate near the radar, and is increased to a nominal level for echoes that originate at large distances from the radar. Figure 5 shows an example of an STC curve for an air surveillance radar. Although some interference energy might fall below the STC noise threshold for close-in targets, STC is not, per se, a radio interference suppression mechanism.

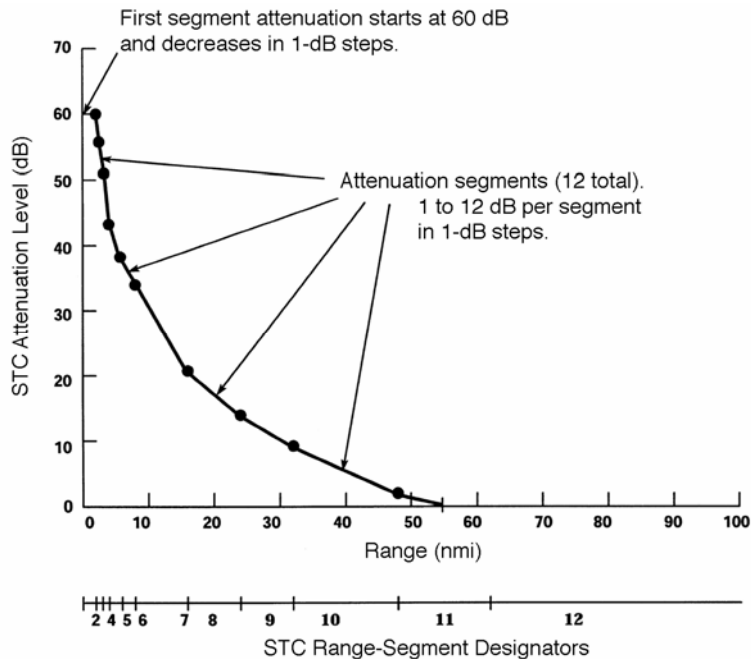


Figure 5. Example STC curve for an air surveillance radar.

### 1.10.2 Log Fast Time Constant (Log-FTC or FTC) and Comparison with STC

Another important method for reducing the effect of clutter echoes is *log fast time constant* (log-FTC, or simply FTC). FTC log-compresses the dynamic range of clutter energy [12, pg. 77] and therefore reduces the variation in clutter levels at the receiver output. This effect, in turn, results in a relatively constant false alarm rate (CFAR) with a somewhat inexpensive implementation in the radar design. CFAR is described in more detail below.

FTC works if the input clutter (or noise) is described by a Rayleigh probability density function. Sea clutter and land clutter are non-Rayleigh, and thus log-FTC is not so effective against them. But FTC works well against precipitation clutter, and is sometimes called a *weather fix* [9, pg. 506-507].

The effect of FTC is somewhat like automatic STC, but unlike STC it does not suppress clutter entering the radar receiver through the antenna sidelobes. (Because STC reduces gain when the transmitted radar pulse energy is still at close distances, it does work against echoes entering through the sidelobes.) If clutter is strong enough to be received through the sidelobes it may not be adequately reduced by the log effect of FTC. Therefore, STC and logarithmic receivers are sometimes used together, with the STC working in the RF part of the receiver and the logarithmic amplifier working in the radar IF section.



STC is range-dependent, while log-FTC is range-independent. Neither technique improves the ratio of target-to-clutter power. The benefits of FTC are traded against some loss in the probability of detection of targets. FTC is not a radio interference-suppression feature.

### **1.10.3 Instantaneous Automatic Gain Control (IAGC, or AGC)**

*Instantaneous automatic gain control* (IAGC, or simply AGC) is yet another technique for avoiding overload of radar displays by strong clutter blocks. AGC works through a negative-feedback loop between the IF amplifier output and the gain control of that circuit [12, pg. 78]. The time constant of the AGC is set to a long interval, so that extended clutter effects are reduced, while the short-response time responses due to echoes from discrete targets are not affected. AGC is commonly implemented in aircraft-tracking radars that implement conical beam-scanning and monopulse tracking techniques [9, 11]. The AGC filter loop is a low-pass design that passes frequencies from dc to just below the antenna beam-scan rate, thus assisting tracking capabilities.

AGC causes reduction in receiver sensitivity in the presence of strong signals and thus mitigates radar display overload, but it also decreases the probability of detection of undesired targets. It is therefore not an interference mitigation technique.

### **1.10.4 Constant False Alarm Rate (CFAR)**

A simple form of analog constant false alarm rate (CFAR) processing was discussed in Section 1.10.2 in connection with log-FTC circuitry. CFAR is often an optional feature for many simple, analog radar displays, but its implementation is often essential for digitally processed radar signals [12, pg. 98]. The reason for the discrepancy is the intelligence that human operators bring to the problem of interpreting radar plan position indicator (PPI) displays, versus the inherent limitations of digital processing algorithms relative to human intelligence. Human operators can become skilful at distinguishing true targets from noise and clutter artifacts on such displays, and if too many false targets (false alarms) are occurring, then the operator can reduce the gain setting of the PPI display—in effect providing an approximation of automatic CFAR, albeit with a relatively slow response time [12, pg. 99].

But in automated detection and tracking systems, where the design goal is to automatically designate targets and display them, the processing algorithm can be overwhelmed by too many false targets. (A change of only 1–dB in the threshold-to-noise or threshold-to-clutter ratio can change the false alarm rate by 2 orders of magnitude [12, pg. 99]. Thus an automatically adaptive CFAR technique is therefore essential for such radars.

In a typical CFAR implementation, a test cell is designated. Around that cell, a group of tapped digital delay lines are used to estimate the average level of noise or clutter. The tap outputs (usually 16 to 20) are summed, the sum is multiplied by an appropriate constant, and the result is used to set the detection threshold for the test cell [12, pg 99, and 9, pp. 392-395]. The output of the test cell is the radar output. This approach is called *adaptive video thresholding*.

Additional variations of CFAR exist [9, pg. 394]. One of these is a post-detection integrator (a low-pass filter) that is used to estimate average noise, the output then being fed forward to control the detection threshold. Another technique, called the *Dicke fix*, is to use a broadband IF filter followed by a hard limiter and a narrow matched filter. The hard limiter is set low enough to limit receiver noise. But signal energy causes the output of the matched filter to increase by a factor that is equal to the ratio of the bandwidths of the wideband and narrowband filters. A variant of this approach uses limiters to discriminate between desired target echoes and interference by observing the change in time of the phase pattern at the limiter output [17, pg. 3.49]. The limiter output is correlated with phase-coded information in the transmitted waveform; the better the correlation, the more likely the energy is a target echo. This approach, called *phase-discrimination CFAR* or *coded-pulse anticlutter system* (CPACS), destroys all amplitude information in the echo returns.

CFAR processing has a number of drawbacks. It causes losses relative to optimum detection, and the number of pulses that are required for processing must be large to minimize this loss. CFAR inevitably reduces the overall probability of detection of desired targets, and thus will cause some targets to be lost. These losses can be insidious because operators will often be unaware that CFAR-controlled detection thresholds are gradually creeping upward as noise, clutter, or interference increase in some environment [9, pg 395; 12, pg. 99]. In CFAR radars, anti-interference measures should therefore be implemented (if any are available) ahead of the stage where CFAR processing occurs.

In summary, CFAR processing is a necessary evil that suppresses clutter and noise effects at the cost of losing some desired targets. CFAR will suppress interference from low duty-cycle (less than a few percent), asynchronously pulsed sources (i.e., other radar transmitters). But CFAR does not function as an anti-interference technique for higher duty-cycle (i.e., non-radar) signals. In fact CFAR can make the effects of high duty-cycle interference worse by insidiously suppressing desired targets in the presence of such interference without any awareness of the problem on the part of radar operators.

#### **1.10.5 Interference Rejection (IR)**

As described in [18], many radar designs include an operator-selectable feature called *interference rejection* (IR). The purpose of IR is to reject or suppress interference into a radar receiver from co-channel transmissions from *other radars*. For reasons that will presently become clear, IR is not effective against non-radar (communication-type) signals. IR is especially useful in radar bands in which large numbers of radars are tuned to the same frequency; two of these cases are 3050 MHz, a popular frequency for S-band maritime radionavigation radars, and 9400 to 9410 MHz, a popular range for the tuning of X-band maritime radionavigation radars. Without the IR feature activated, the effect of interference from multiple, co-channel radars is shown in Figure 6.

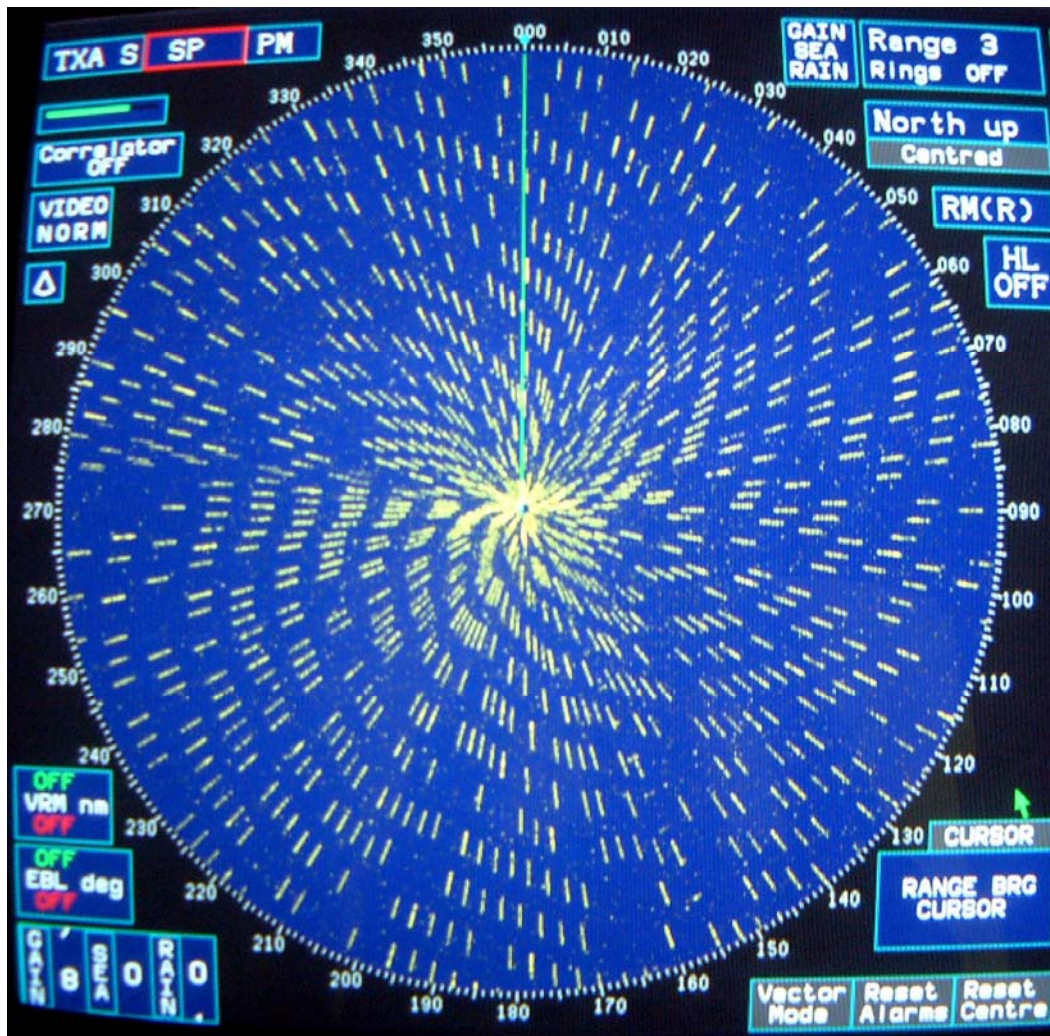


Figure 6. An example of continuous severe co-channel radar interference on a PPI display. The average  $I/N$  level of the interference is 0 dB and the IR and STC features are switched off. IR circuit designs are often protected as trade secrets, but there are at least two broad approaches that work on two different principles of pulse-to-pulse correlation: Pulse repetition interval (pri) discrimination, and pulse width (pw) discrimination [18].

A block-diagram for the pri discrimination IR design is shown in Figure 7. In this approach, echo pulses in the radar video section are passed through a threshold comparator and then through two channels via a splitter. In one channel the pulses are delayed by the pulse repetition interval and in the other channel there is no net delay relative to the first channel. The two resulting outputs are then ANDed. If the echo intervals match the radar transmitter pri, then the AND gate output goes high; otherwise the AND output goes low; the AND gate condition is used to pass video data. The result is that radar pulse sequences that do not match the transmitter pri are suppressed at the video output. Note that one of the input pulses is lost, and that low-amplitude echoes are discriminated against. Also, this technique does not enhance desired signals, but only suppresses undesired signals.

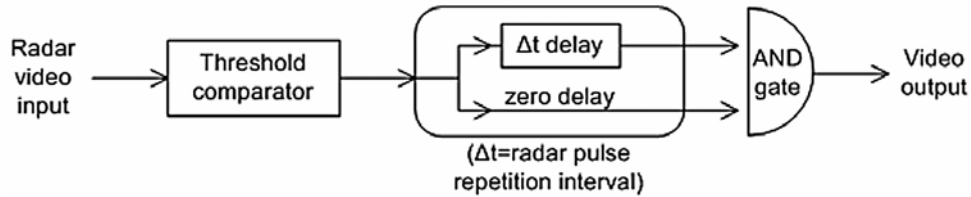


Figure 7. Pulse repetition interval (pri) interference rejection circuit block diagram.

A somewhat similar conceptual approach is used for pw discrimination IR. In this design, the input pulses are differentiated and split into two channels. In one channel the differentiated pulses are delayed an interval corresponding to desired pulse width,  $\tau$ , while in the other channel the differentiated pulses are inverted. If an input pulse is of width  $\tau$ , the differentiated trailing edge inverted pulse will coincide in time with the leading edge pulse delayed in time  $\tau$ . The coincidence circuit passes signals in the two channels only if they are in time coincidence; if an input pulse is not of width  $\tau$ , the two spikes will not be coincident in time and the pulse is rejected. This technique results in reduced receiver sensitivity and probability of target detection. Figure 8 shows a radar display (with radar interference present) when IR is deactivated versus activated.

In addition to pulse-to-pulse IR techniques, some radars also incorporate IR that works on a scan-to-scan basis. This feature operates by using a memory of apparent targets that is either reinforced (or not) from one scan to the next. Since false targets generated by stray pulses from other radar systems will not be expected to occur at the same location on the PPI display from one scan to the next, such targets may be dropped from the display if no reinforcement occurs on a scan-to-scan basis. Targets that do continue to occur at the same location on the PPI display (or at nearly the same location, within some specified bounds of translational movement) are remembered from previous scans and continue to be displayed.

The IR feature in radar receivers only works against low duty cycle, pulsed, asynchronous interference. The use of IR is a necessary evil for radar operations, because it causes some targets, especially ones that are weak, to be lost. For pulse-to-pulse IR techniques, losses occur due to the comparator threshold setting (in the pri IR design) and because of the reduced number of pulses that are available for data processing and overall reduced receiver sensitivity with these circuits. For scan-to-scan IR processing, weak targets that tend to fade out normally in a high percentage of scans will be lost because of their intermittent behavior. IR is not effective against communication-signal interference because such interference is normally of much higher duty cycle than radars. Appendix A expands on the results of IR performance studies that were performed in conjunction with the test effort described in this report.

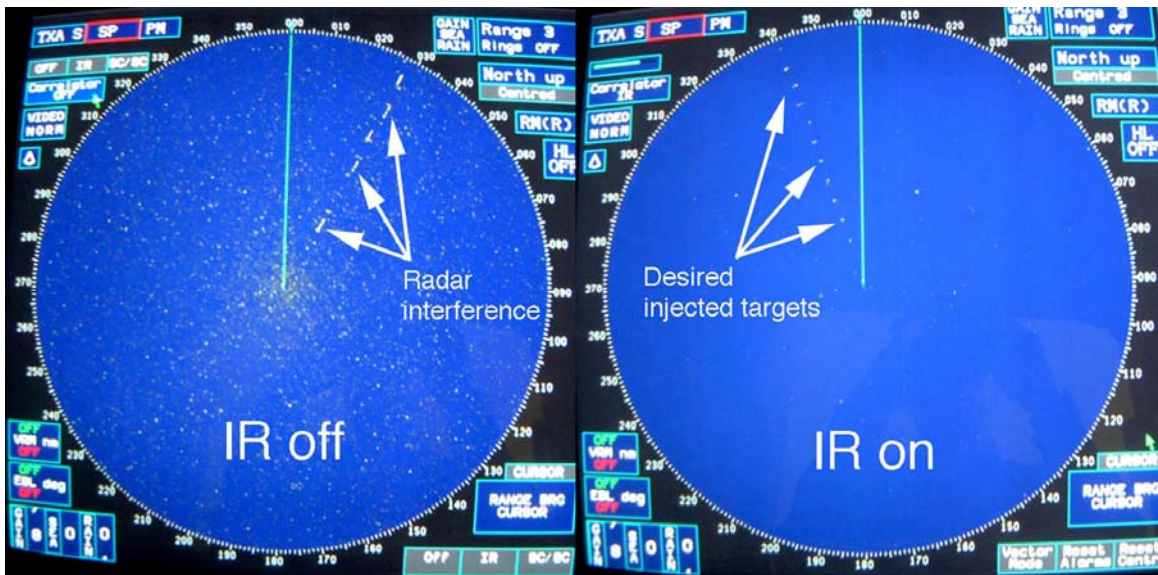


Figure 8. Radar display with IR turned ‘off’ versus ‘on’ in the presence of interference from other, gated radar-like pulses. A set of ten desired targets has been injected in both images, at 30 degrees azimuth at the left and at 340 degrees azimuth on the right. The targets are obscured by coincident radar interference when the IR is turned off (left), but are easily visible through the same interference when the IR feature is activated (right). IR has been found to be effective only for low duty-cycle (less than about 1-3 percent) interference, such as generated by radar transmitters.

## 2 SETTING CONDITIONS FOR INTERFERENCE MEASUREMENTS ON RADAR RECEIVERS

For tests and measurements of radar receiver performance in the presence of RF interference, it has proven crucial to establish baseline conditions for the operation of the radars and the injection of interference into the receivers. The basic baseline conditions and parameters are described here. Additional and more detailed descriptions of the test conditions are provided in later sections of this report, in connection with the discussion of tests and measurements on the individual radars in this study. Figure 9 shows the typical appearance and conditions of a radar station control console and PPI display.



Figure 9. Typical conditions inside an air-search radar station, showing the main console for display and control.

### 2.1 Interference Coupling Technique

It was essential that the levels of interference in each radar receiver be quantified as precisely as possible. Such quantification is difficult or impossible if interference is coupled radiatively into the radar receivers. Radiative coupling also introduces problems with spectrum coordination with other agencies. There is also always a chance that other signals in the vicinity of the radar might cause some sort of additional interference in the receiver. Taking all of these factors into

consideration, interference signals were injected into all of the radars in this study via hardline couplings, with desired targets likewise injected at the RF front end via a combiner. The typical test configuration is shown in Figure 10.

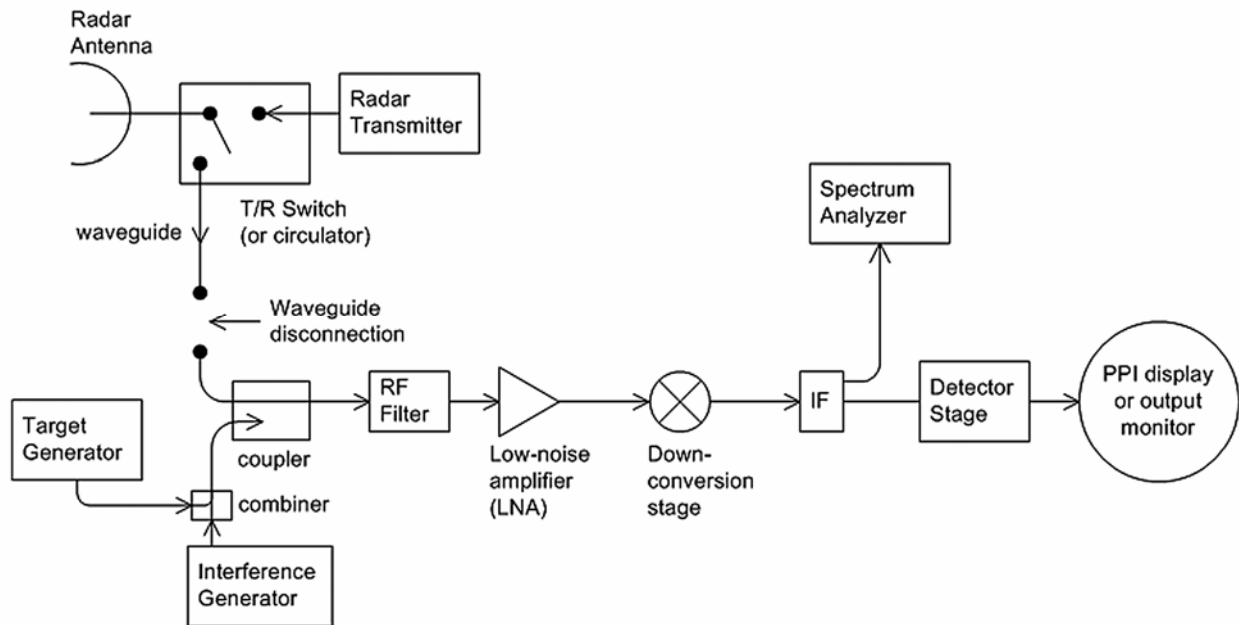


Figure 10. Block diagram of a typical test configuration in this interference study. Interference and desired targets were generated at radio frequencies and were injected at the radar receiver RF front-end ahead of the first RF filter and LNA. The spectrum analyzer is an external, diagnostic test and measurement accessory that is tapped from the IF via a directional coupler.

The hardline connections for interference were always made at the radar RF front end, as close as possible to the radar antenna, with the radar running in a receive-only mode. In particular, the RF interference was fed into the radars *ahead* of the first RF low noise amplifier (LNA). Thus the receivers were subjected to RF interference that replicated energy that would have otherwise been fed into the receivers via the radar antennas. This approach ensured that all sections within the radars behaved normally, the same way that they would have if the interference had been radiated normally into the radar units.

For the second model of long range air route surveillance radar, as described in Section 3, the first RF low-noise amplification section consisted of a distributed array of LNAs built on a feed platform in front of the antenna reflector; it was mechanically impossible to couple the RF interference into this array in such a way as to feed all of the LNAs. Instead, a hardline connection was made to the input of the first RF stage ahead of a selected LNA on a selected element row of the array.

## 2.2 Calibration of Interference Levels

Whenever possible, the relative levels of interference,  $I$ , and receiver noise,  $N$ , were directly measured as  $I/N$  ratios within the IF section of each radar. Figure 11 shows NTIA and FAA engineers assessing such an IF tap point. When no access was available to a radar's IF section, then the radar receiver noise figure was measured and the  $I/N$  levels were computed. Procedures for both the direct observation method and the indirect computation method are provided here.



Figure 11. NTIA and FAA engineers determining the locations on a radar IF-stage circuit card where the  $I/N$  level could be monitored.

In all of these  $I/N$  calibration procedures, it is critical to distinguish between cases in which the interference bandwidth exceeds the radar IF bandwidth (wideband) versus cases in which the interference bandwidth is less than or equal to the radar IF bandwidth (narrowband). The critical difference between these two cases is that all of the power generated for narrowband interference will be coupled into the radar IF, whereas only a fraction of wideband interference power will contribute to the  $I/N$  ratio, and account must be taken of that offset (called on-tuned rejection, or OTR) in the effective value of  $I$  in the receiver IF stage.



### 2.2.1 $I/N$ Calibration with Access to the Radar IF for Non-Pulsed Signals

In cases where access to the radar IF was available, the technique for determining  $I/N$  levels was to first connect a spectrum analyzer with average detection to the radar IF output and observe the radar noise power level in a resolution bandwidth (RBW) matched as closely as possible to the radar IF bandwidth. Then the interference generator output was fed into the radar RF front end input and the interference power was adjusted until it caused an increase of 3 dB on the spectrum analyzer display. Since the spectrum analyzer display showed the quantity  $[I/(I+N)]$ , this meant that  $[I/(I+N)]=3$  dB, implying that  $I=N$  and therefore  $I/N=0$  dB. With this method, all  $I/N$  levels were referenced to the indicated  $I=N$  level. Figure 12 shows an example of the IF output for this approach.

Because the interference level was directly monitored in the radar IF bandwidth, no special account needed to be taken of the  $I$  power level if the interference bandwidth exceeded the bandwidth of the radar IF. Whatever the amount of OTR that might occur due to the bandwidth difference, the direct observation of a 3-dB increase in the IF at some interference power generator setting provided assurance that the corresponding setting of the generator output panel was in fact creating a 0-dB value for  $I/N$  in the radar IF bandwidth.

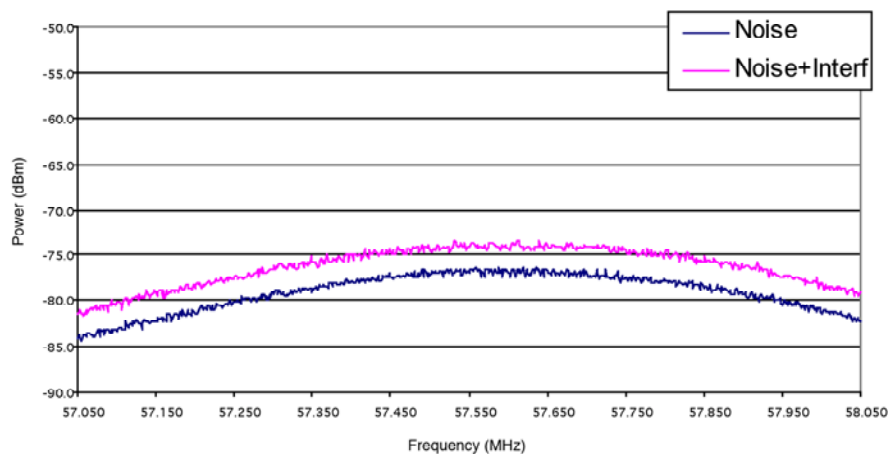


Figure 12. Example of a 0-dB  $I/N$  calibration noise spectrum (57.55 MHz IF frequency). Interference is wideband CDMA (W-CDMA). The noise-plus-interference curve is 3-dB higher than noise-only curve.

### 2.2.2 $I/N$ Calibration with Access to the Radar IF for Pulsed Signals

For tests in which pulsed interference was injected, the level of the pulsed interference was adjusted until the peak power from the pulses was observed 20 dB above the receiver IF level. In that case,  $[I/(I+N)]=20$  dB, implying that  $I/N$  was virtually 20 dB. (Care was always taken to be sure that the pulse peak power level was measured in a bandwidth that was wider than (1/pulse width) to ensure that all pulse power was convolved into the measurement.) This approach is depicted in Figure 13. With this method, all interference  $I/N$  levels were simply referenced directly to the level that gave an indicated  $I/N$  of 20 dB in the receiver IF stage.

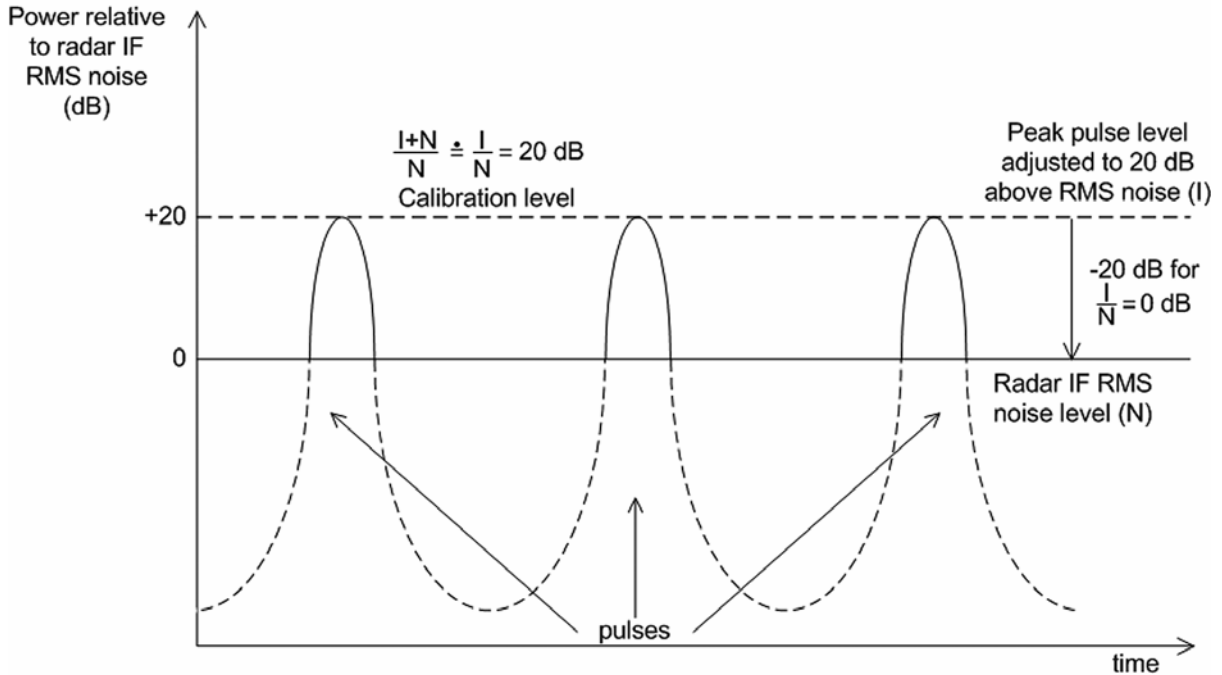


Figure 13. Calibration technique for pulsed interference. Peak pulse power is measured in a bandwidth exceeding  $(1/\text{pulse width})$ , and peak power for all subsequent testing is referenced to the injected level where  $[(I+N)/N]=20$  dB, which differs from  $I/N=20$  dB by only 0.04 dB, well within the uncertainty of the measurement itself.

Although pulsed signals would generally produce emission bandwidths that would be wider than the radar IF bandwidth, the OTR factor due to the bandwidth offset was physically incorporated into the observation of effective interference power in the radar IF stage. Thus the direct observation of the effective  $I/N$  level in the radar IF stage obviated any need to compute an OTR factor for such interference; the signal generator setting that produced a 20-dB increase relative to the radar IF noise floor was in fact the setting that produced a true  $I/N$  level of 20 dB.

The analysis above only applies if it is possible to match the spectrum analyzer resolution bandwidth (RBW) to the radar IF bandwidth. If it is impossible to make the spectrum analyzer IF bandwidth match the radar IF bandwidth, then the  $I/N$  at the radar IF output is determined by taking into account the OTR:

$$\left(\frac{I}{N}\right)_{IF} = \left(\frac{I}{N}\right)_T - OTR \quad (9)$$

where:

- $(I/N)_{IF}$  = interference to noise ratio in the bandwidth of the radar IF stage;
- $(I/N)_T$  = interference to noise ratio that would occur if the radar IF bandwidth were equal to or wider than the bandwidth of the RF interference produced by the transmitter;
- $OTR$  = on-tuned rejection factor.

For CW-like signals, the OTR factor is given by:

$$OTR = 0 \text{ for } B_{IF} \geq B_T \quad (10a)$$

$$OTR = 10\log(B_T/B_{IF}) \text{ for } B_{IF} < B_T \quad (10b)$$

where:

$B_{IF}$  = radar receiver IF 3-dB bandwidth (Hz);

$B_T$  = transmitter 3-dB bandwidth of the interference signal (Hz).

During the measurements described in this report, the  $I/N$  ratio calculated above (taken into consideration with the OTR) was noted where applicable, along with any associated attenuation settings. The interference generator power output level and associated attenuation settings that produced an  $I/N$  ratio of 0 dB at the radar IF output was recorded, and other  $I/N$  values were obtained by adjusting the interference attenuator setting.

### 2.2.3 $I/N$ Calibration without Access to the Radar IF

Almost all radars used in this study were accessible at their IF stages. But in the rare cases in which no access to the radar IF stage was available, an indirect  $I/N$  calibration method based on the specified radar noise figure and 3 dB IF bandwidth was used; radar noise figure and radar IF bandwidth were taken from documentation.<sup>12</sup>

Thermal noise at room temperature (about 290 K) is  $kTB = -114$  dBm/MHz. The receiver inherent noise level (in dBm)  $N$ , at the receiver IF output referred to the receiver RF input is given by:

$$N = -114 \text{ dBm/MHz} + 10\log(B_{IF}) + NF \quad (11a)$$

or

$$N = -168.6 \text{ dBm} + 10\log(B_{IF}) + 10\log(T) \quad (11b)$$

where:

$B_{IF}$  = receiver IF bandwidth (MHz);

$NF$  = radar receiver noise figure (dB);

$T$  = radar receiver effective noise temperature (K).

For example, suppose that a radar operated with a 100-ns pulse width. Then a typical IF bandwidth matching that pulse would be  $(1/100 \text{ ns}) = 10$  MHz. A good radar receiver noise figure would be 5 dB. In this case the radar noise power in the IF would be  $(-114 \text{ dBm} +$

---

<sup>12</sup> Radar IF bandwidth would normally be nearly equal to  $(1/\text{pulse width})$  of the radar, and this knowledge was used to help verify that the specified IF bandwidth was sensible.

$10\log(10 \text{ MHz}) + 5 \text{ dB} = -99 \text{ dBm}$  (that would be measured in a 10 MHz RBW). In other values of RBW, the measured noise power in the radar IF would vary as  $10\log$  of this value.

The OTR complication (already described above) arises for interference signals with bandwidths that are wider than the radar IF bandwidth. Extending the example above, suppose that an interference signal that has noise-like characteristics (such as code division multiple access (CDMA)), and which thus varies in power as  $10\log(\text{RBW})$  is to be injected into the radar RF front end. The complication arises because the radar IF is too narrow to convolve all of the power in the interference signal; in effect, the radar sees only a fraction of the interference power, that fraction being given by an OTR ratio  $10\log(B_{\text{interference}}/B_{\text{IF}})$ .

Suppose, for example, that the CDMA signal bandwidth were 20 MHz and the goal is to inject this signal into the radar with a 10 MHz IF bandwidth at an  $I/N$  ratio of 0 dB. The nominal 0-dB signal generator power output level would in this case have to be increased by the OTR amount of  $10\log(20 \text{ MHz}/10 \text{ MHz}) = +3 \text{ dB}$ . Account would also have to be taken of all losses between the signal generator and the RF injection input point, which would typically be on the order of 15 dB loss. The resulting 0-dB  $I/N$  is calculated by the equation:

$$P_{gen} = P_{noise} + OTR + P_L \quad (12)$$

where:

- $P_{gen}$  = power output (panel display level) from the interference generator, dBm;
- $P_{noise}$  = radar IF noise power level in the bandwidth of the radar IF (dB);
- $OTR$  = on-tune rejection factor  $10\log(B_{\text{interference}}/B_{\text{IF}})$  dB;
- $P_L$  = loss between the signal generator output and the radar RF front end input, dB.

Suppose for example that  $P_{noise} = -99 \text{ dBm}$  in 10 MHz;  $OTR = 10\log(20 \text{ MHz}/10 \text{ MHz}) = +3 \text{ dB}$ ; and  $P_L = 15 \text{ dB}$ . Then  $P_{gen} = -99 + 3 + 15 \text{ dB} = -81 \text{ dBm}$  displayed power output from the interference generator for an  $I/N$  level of 0 dB. All other values would follow from this, as shown in Table 1. It should be noted that, in this method, *all* losses and gains between the interference generator output and the radar RF front end input must be carefully measured.

Table 1. Example of Interference Power Levels When Interference Bandwidth Exceeded Radar IF Bandwidth

<b><i>I/N</i> (dB)</b>	<b>Path Loss (dB)</b>	<b>Radar IF Bandwidth (MHz)</b>	<b>Interference Signal Bandwidth</b>	<b>OTR (dB)</b>	<b>Interference Signal Generator Panel Display (dBm)</b>
-6	15	10	20	+3	-87
-3	15	10	20	+3	-84
0	15	10	20	+3	-81
+3	15	10	20	+3	-78
+6	15	10	20	+3	-75

## 2.2.4 Setting $I/N$ Levels from Calibration Data

For all calibration techniques, the various levels of interference were subsequently adjusted to particular values by attenuating the input relative to the calibrated level. For example, suppose that the panel display power value that gives  $(I+N)/N = 3$  dB is -84 dBm. This becomes the 0-dB  $I/N$  point. Then a 3-dB reduction in the interference level relative to that point would be an  $I/N$  level of -3 dB, which would occur at -87 dBm output power from the generator. An example of a complete conversion table as used for typical radar interference measurements is shown in Table 2.

Table 2. Example of Interference Power Levels When Interference Bandwidth was Less Than or Equal to Radar IF Bandwidth

$I/N$ (dB)	Interference Signal Generator Panel Display (dBm)
-10	-94
-9	-93
-6	-90
-3	-87
0	-84
+3	-81
+6	-78

## 2.3 Injection of Desired Targets

All of the radars that were tested were designed to detect and display discrete targets, with the exception of a meteorological (weather surveillance) radar. Degradation effects needed to be assessed based on target detection effects (loss of targets versus false targets). Therefore it was critical to ensure that a useful set of baseline targets were provided at all stages of testing on each radar receiver. For most testing, the need for a good set of baseline targets was met by injecting a hardline-coupled set of  $n_{target}$  fixed-amplitude pulses, the number of pulses being:

$$n_{target} = \left( \frac{\theta}{360} \right) \left( \frac{T_{scan}}{pri} \right) \quad (13)$$

where:

- $n_{target}$  = number of pulses injected for each target;
- $\theta$  = 3-dB radar antenna azimuthal beamwidth (degrees);
- $T_{scan}$  = time required for a 360-degree radar antenna scan;
- $Pri$  = pulse repetition interval (sec).

For example, if a radar with a 1-degree beamwidth generated 1000 pulses per second (for a pri of 0.001 sec) and had a scan interval of 4.75 sec, then  $n_{target} = 13$  (rounded to the nearest integer).

The injection was done at the radar IF frequency. Usually a set of ten targets were injected in this way. Figure 14 shows the target and interference injection equipment typically transported by NTIA engineers to a radar station. Figure 15 shows a block diagram of the target-generation hardware developed for the study; additional hardware was used to synchronize target injection with radar PPI scan triggering.



Figure 14. Typical arrangement of NTIA interference and target generators at an air search radar station. The NTIA equipment is spread across the table in the foreground and the cart in the background, with the radar PPI display at right.

The set of desired targets was injected on every radar scan.<sup>13</sup> In most tests the targets were injected synchronously with a scan trigger from the radar set, thus keeping the targets at fixed locations on the radar PPI displays from scan to scan.<sup>14</sup> In tests in which scan synchronicity was not possible to achieve, target positions shifted a few degrees in azimuth from one scan to the next.

On each scan, at least ten equally spaced test targets were usually injected at equal power levels in a sequence that placed them radially on the radar PPI display, as shown in Figure 16.<sup>15</sup> For real targets, this radial distribution would imply a change in distance between the radar site and the

---

<sup>13</sup> In this report, “scan” means a single, 360-degree rotation of the radar beam.

<sup>14</sup> For a few radars, no such trigger was available and operator-adjusted synchronous timing was used instead.

<sup>15</sup> In some tests, a set of four such radials were injected during each scan at angular intervals of ninety degrees, providing forty targets per scan.

targets, with a concomitantly increasing cross section with distance. But for the purpose of the NTIA test and measurement series, this arrangement was *not* meant to replicate effects due to changes in distance. Instead, it was simply an expedient to ease the difficult process of counting targets during interference runs; radially distributed targets were found to be easier to count than equal-radius, sector-distributed targets.

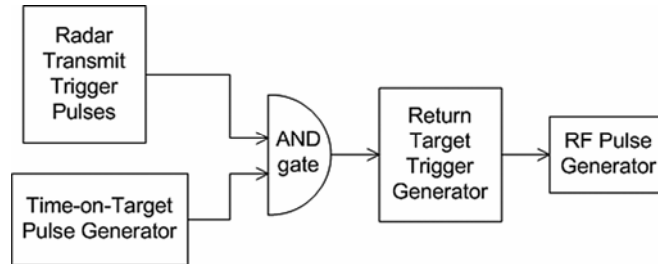


Figure 15. Block diagram of the radar target-generation hardware developed and used for the study.

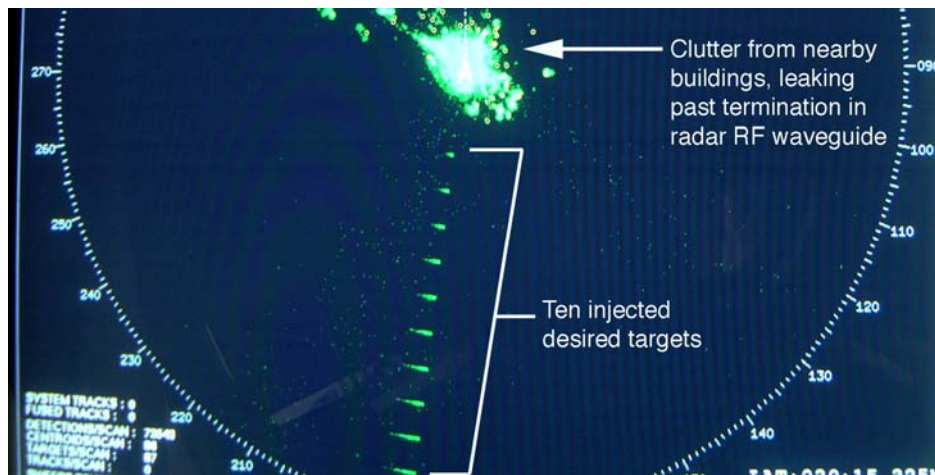


Figure 16. Example of a maritime radar PPI display during interference testing with ten injected targets on a single radial. Clutter condition was used diagnostically to verify proper radar operation.

One radar, a long-range air surveillance system, incorporated a built-in target generator and an automated target counter; NTIA engineers took advantage of those features during the testing. Those targets were displayed throughout sector wedges on the PPI display as shown in Figure 17, but again the target cross sections were constant; no distance effects were incorporated. As was the case for the NTIA-generated targets, the radar PPI display arrangement in sector wedges was simply a convenient way for the system software to arrange the targets on the screen.



Figure 17. Sector-wedge distribution of desired targets on a PPI display during testing on a long-range air search radar. Targets are shown as “+” signs, and are generated at the radar RF stage.

Some live-target testing was done within range of a busy airway with a long-range air surveillance radar in the Midwestern area of the US. Although a test phase at that radar included the use of standard NTIA-generated desired targets, the live-target phase of the testing allowed the observation of interference effects against actual aircraft in flight, ranging from commercial airliners to small airframes.

For meteorological radar tests and measurements, discrete targets could not be used because those radars are designed to monitor extended atmospheric phenomena. For those tests, actual weather echoes and radar internal noise were used in the course of the test program, as described more fully in Sections 5 and 7.

## 2.4 Use of Fluctuating Versus Non-Fluctuating Targets in Radar Testing

The question naturally arises whether tests of the effects of low-level interference in radar receivers should be performed with constant amplitudes for the desired targets, versus against desired targets with fluctuating levels. It can be argued that fluctuating targets might resemble real-world targets most closely, and thus should be used. But this argument has been found to be incorrect. The reasons are as follows:



- 1) Real targets do not fluctuate in accordance with the mathematical models (called Swerling models or cases [9, pp. 46-52]) that are used to design microwave radars. There is no general-purpose mathematical description of target fluctuation that works for a general class of radar targets under all operational conditions. The Swerling models are used because they are analytically tractable and provide some resemblance to the range and rate of variation that might be seen in some real targets.
- 2) Although radars are designed to use a sufficient number of pulses per target per scan to accommodate some amount of target-power fluctuation, this does not necessitate the use of power fluctuations during testing of radar performance. Rather, testing can be just as well performed against a fixed, *nominal* target power level. Such a level would represent the behavior of many real targets, which have been observed by the authors to fluctuate little or not at all from one scan to the next in many cases.
- 3) During testing, radar receiver performance must be compared in two conditions: interference being present versus no interference being present. A meaningful comparison of these two conditions means that a baseline target detection performance level must be established when no interference is present. Experience of NTIA engineers has shown that such a baseline is easy to establish if target power level in the receiver is held constant, but is difficult to achieve if target power levels fluctuate about that nominal value in accord with the Swerling models. The problem is that, if the target power fluctuates according to, for example, Swerling case 1 [9, pp. 46-47], then (roughly) half of the targets nearly burn the phosphor on the PPI display, while the other half (roughly) are simply absent. Therefore the baseline level of detection becomes approximately 50% for such targets. But meaningful performance tests need to be performed with a target probability of detection that is closer to 90%. To achieve 90% performance with Swerling case 1 fluctuating target distributions, as shown in Figure 18, the *mean value of the fluctuating targets must be increased by perhaps 10 dB or more*. This approach would be problematic because it would be equivalent to compensating for target fluctuations by turning up the radar transmitter power by 10 dB, which is exactly what operational radars *cannot* do to enhance target returns. Furthermore, if this step is taken with a target generator in actual testing, then most of the target returns nearly burn the phosphor on the PPI, which again is not a realistic scenario.
- 4) Observation of genuine targets, both aircraft and boats, by NTIA engineers indicates that non-fluctuating test targets more nearly resemble the behavior of real targets on radar PPI displays. Furthermore, non-fluctuating test targets can be adjusted to a 90% probability of detection and that level can be used as a reliable baseline through all testing on a radar unit.

For all the reasons above (maintenance of a constant non-interference performance baseline, replication of the behavior of genuine airborne and maritime radar targets, and overall practicality of testing), NTIA testing has mostly used constant-amplitude test targets that are held at a power level at which they are detected 90% of the time on the radar PPI display when no interference is present. An exception has been made for meteorological radars, which do not detect discrete targets, and in which actual atmospheric echo returns have been used.

It is worth noting that by setting the probability of detection of the test targets to 90%, NTIA engineers provided substantially stronger target levels for the radar receivers than might have been justified by the 80% probability of detection criteria that many reference sources [9-14 and 19] quote for purposes of adequate radar design. The two probabilities might not be comparable because setting a design criterion is not the same as setting an interference-test performance criterion. The purpose of the NTIA tests and measurements was to determine upper limits for interference levels that produce deleterious effects in radar receivers. In other words, the purpose was to test interference effects against targets that were undoubtedly high-quality, but still within the range of credibility for real radar echoes. If an interference level with some modulation was found to affect the detection of targets that had a 90% probability of detection in the absence of interference, then the detection of almost any real targets by the same radar receiver would be expected to be adversely affected by the same interference level of that modulation. Put another way, with 90% probability of target detection in the absence of interference, the tests were structured in the direction of accepting higher rather than lower levels of interference before radar receiver performance was adversely affected.

#### 2.4.1 Overview of Fluctuating Target Level Generation

Even considering all of the arguments above, some interference tests were performed on a maritime radar with fluctuating targets. Those test procedures and their results are specifically described in Section 6, but an overview of the fluctuating target approach is as follows.

As seen in Figure 18, the behavior of logarithms causes the values in each distribution to naturally be below 0 dB (and further below 0 dB) more often than they are above 0 dB. This is consistent with the physical reality that reflected power levels from radar targets may increase only a finite amount *above* an average, but may be reduced by an infinite amount *below* an average.

A baseline  $P_d$  curve needs to be determined without any interference being present and with the target power levels fluctuating. To assess the effects of interfering signals when the targets are fluctuating, the  $P_d$  is determined when the I/N level is set to an array of values such as: -9 dB, -6 dB, -3 dB, 0 dB, +3 dB, +6 dB, and so on. This approach allows the fluctuating target baseline  $P_d$  to be compared with the steady target power  $P_d$  and just as importantly allows comparison between the  $P_d$  when the targets are at a fixed power level at some I/N level to the  $P_d$  when targets are fluctuating under the same I/N condition. A key element is to use the same fluctuating target power levels with and without the presence of interference signals.

In choosing target fluctuation values for the tests, the lower part of Figure 18 can be used to select the decibel power values relative to the median target power level, which is 1.6 dB below the mean value. The rationale for this offset can be gleaned from standard texts [e.g., 17, pg. 46-52]. The set of test values are then selected from the curve. For example, the -5.5 dB value has a cumulative probability of about 0.175. So if the target power that gave  $P_d=0.90$  was -75 dBm from the testing signal generator, then the value for that cumulative probability would be -80.5 dBm. Twenty fluctuating target values from the curve will be selected from the figure, an example group being listed in Table 3. One value will be selected for each scan. On each scan, all of the injected targets (usually ten) will thus have a common value.

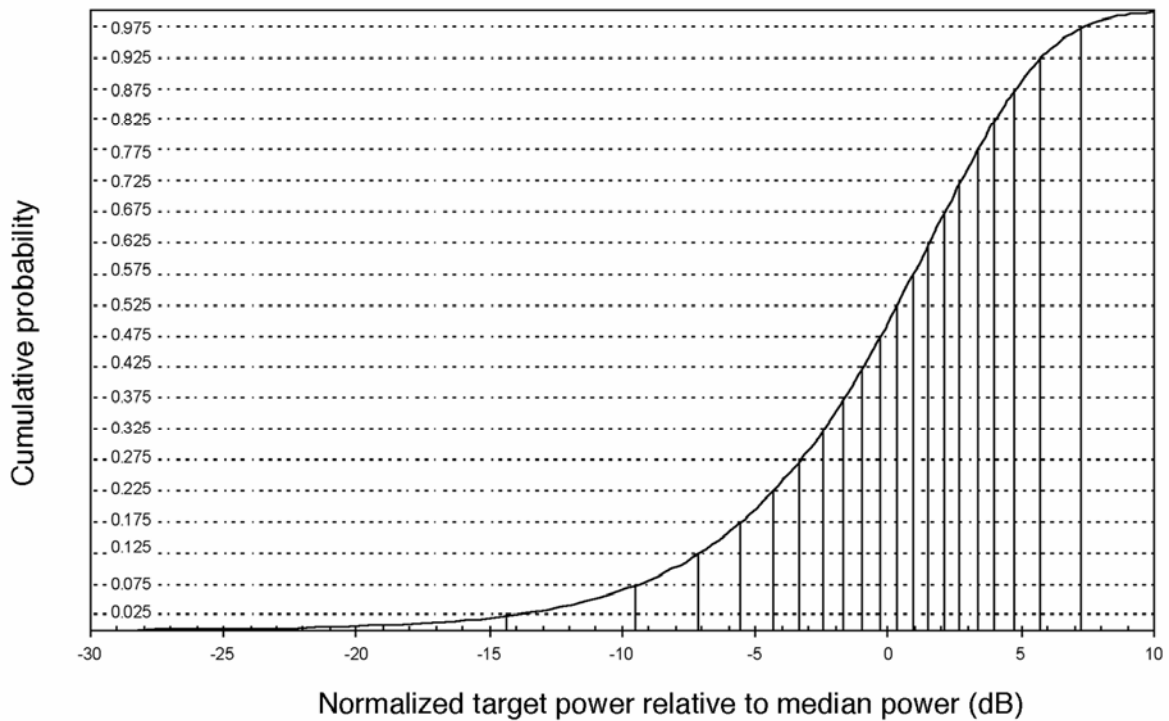
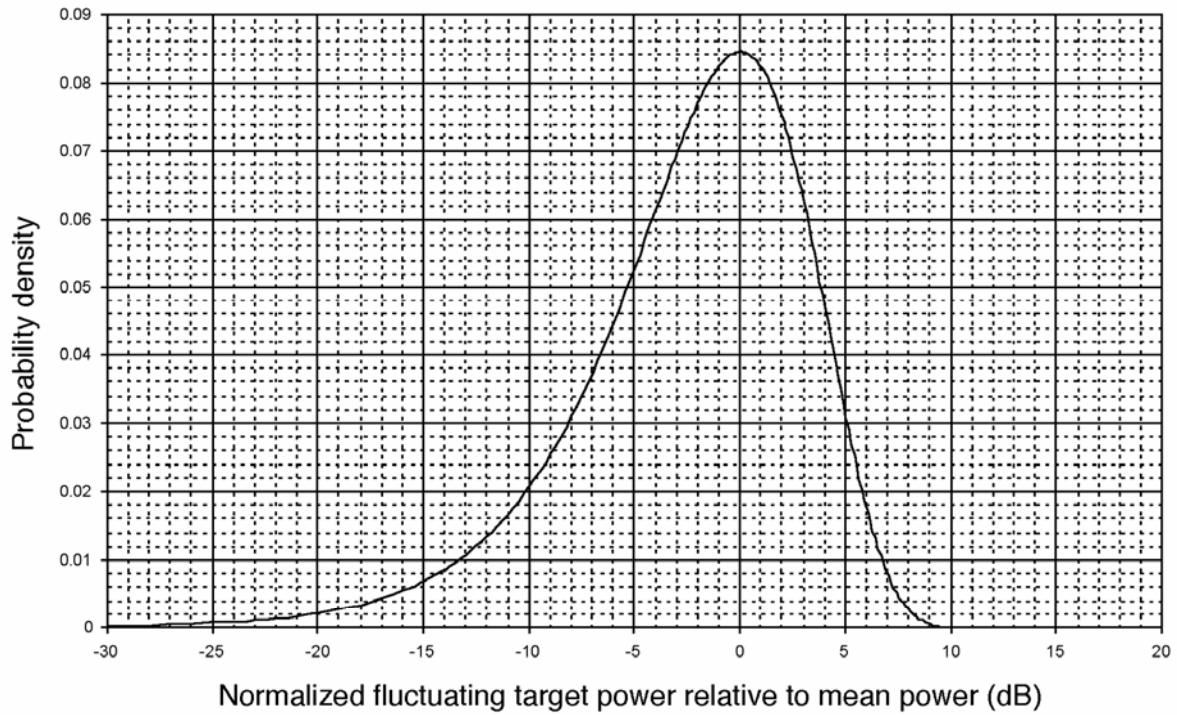


Figure 18. Statistical distributions for Swerling case 1 fluctuating radar target power. If the average level is set to the same value as required for 90% probability of detection of non-fluctuating targets, then most of the targets are not visible on the radar display.

Table 3. Fluctuating Target Power Levels Derived from the Curves of Figure 18

Signal levels (dB) Relative to median power level	
-14.4	0.30
-9.5	0.91
-7.2	1.5
-5.6	2.1
-4.3	2.7
-3.3	3.3
-2.5	4.0
-1.7	4.8
-0.90	5.7
-0.30	7.3

At the end of a test run at a given  $I/N$  level, (usually twenty scans altogether), the total number of observed targets would be divided by the total number of injected targets (say 200) to obtain a single data point for the  $P_d$  of fluctuating targets under the interference condition being tested. Then the interference  $I/N$  level would be changed (its value would be either raised or lowered, or the modulation would be changed), and the entire sequence of fluctuating target levels would be used again for another set of (usually twenty) scans at the new interference level.

#### 2.4.2 Test Methods with Fluctuating Targets

Specifically, the procedure for interference testing with Swerling Case 1 targets was as follows:

First, the zero mean power level for the targets was set to the value that produced a target  $P_d$  of 0.90 without interference present and steady target power levels. Then the variation of the target power level from the value that gave the 90 percent  $P_d$  was chosen from Table 3. The target power was set to that level and the targets were counted. The power of the groups of pulses that defined a target was set to cycle through the twenty entries in the list of power values (relative to the mean value) contained within Table 3. A  $P_d$  count was made by observing the PPI through twenty scans.

Next, the  $I/N$  level was set to one of the following values (-9, -6, -3, 0, 3, 6, 9, 12, 20, or 40 dB) using one of the undesired waveforms and the target generator was cycled through the same varying set of power levels for the chosen sigma; the  $P_d$  was computed for those twenty scans, and so forth.

### 2.5 Target Identification and Counting During Tests and Measurements

Although many radars, including those used in the NTIA test and measurement series, provide automatic target identification and tracking features, NTIA engineers determined during the tests that a human operator (one of the authors, Sanders) was more skilled at identifying and discriminating radar targets than the automated routines built into the radar processors. Many

marginal targets that would be rejected by automated radar processing algorithms were easily identifiable by the human operator, and false alarms were more easily rejected. Most of the tests were therefore run without automated target detection, and the targets that were observed were counted, scan by scan, by the human operator. An additional benefit of using the human operator to identify targets and reject false alarms was that the operator brought the same acceptance criteria to bear on all of the target displays of all the radars in the tests. Figure 16 shows the typical appearance of radar PPI displays under test conditions.

The result was that uniform criteria were applied to target identification on all of the radars (except meteorological, where discrete targets were not used), and the effects of interference were more flexibly allowed to occur before targets were declared to be degraded than would have been the case if automated target identification features had been used. That is, thresholds for the effects of interference were documented at *higher* interference levels than would have probably been allowed if automated processing of targets had been performed. As was the case with 90% probability of detection for targets in the absence of interference, this structured the test results in favor of the occurrence of higher, rather than lower, interference levels before performance degradation was documented.

## 2.6 Radar Receiver Parameter Settings

Every radar used in the NTIA tests and measurements had to be configured for some sort of nominal operation throughout every test series. The most critical settings that had to be considered for all of the discrete-target radars were STC, AGC, and CFAR. (For the meteorological radar, these features were not applicable, and the configuration was adjusted by site personnel who were intimately familiar with the radar behavior, and who adjusted the radar to function nominally in the presence of the local atmospheric and weather conditions.)

Since STC is used to suppress close-in clutter, and since no such clutter could occur due to the hardline-coupled nature of both the RF interference and the injected test targets, the STC feature was normally disabled during radar interference measurements unless otherwise noted in the descriptions of individual tests.

As for AGC, this feature was normally activated during tests in which interference was gated on momentarily during each radar scan, but AGC was deactivated during tests in which interference was continually present during every radar scan. (The first case corresponds to desired target displays on one radial or a few radials, and the latter case corresponds to situations in which the desired targets were displayed in broad sectors throughout radar PPI displays.) AGC was activated for the momentary-interference testing because such interference behavior is expected to replicate ordinary coupling into a radar antenna mainbeam, and AGC could be expected to respond normally (which is to say minimally) to such momentary interference. But in the case of continually-present interference (which would not be expected in the real world except in extreme cases, where the interference would couple strongly into the radar antenna sidelobes), the AGC had to be deactivated because otherwise the AGC feature would decrease the radar gain to a very low value, thereby effectively desensitizing the radar and resulting in the loss of most or all of the desired targets. Such a condition would become a test of AGC behavior rather than of radar receiver performance; the goal of the tests was to determine more inherent system

responses, rather than the response of the AGC feature to interference. (Note, too, that AGC, like STC, is *not* an interference-suppression feature.)

Regarding CFAR, this feature is most useful when automated target identification routines are invoked. It was usually activated during testing because it is used so ubiquitously in the operational modes of most radar receivers. In some cases, CFAR processing can be controlled by manipulating the number of guard cells, but the settings for this feature are usually not changed much during the operational life of most radars.

Considering IR functionality, this feature was sometimes toggled on and off during testing (for radars that incorporated this feature, such as the maritime units) to demonstrate the effectiveness of the IR features in the radar system. Because testing revealed that IR was not effective at high duty cycles, some tests were performed to determine the threshold at which IR functionality was impaired. The behavior of IR in radar receivers is further described in Appendix A.

### 3 INTERFERENCE MEASUREMENTS ON LONG-RANGE AIR SEARCH RADARS

#### 3.1 Introduction

Long-range air surveillance radars routinely search for, and track, airborne targets at distances exceeding 200 nmi. They sometimes incorporate meteorological (weather) surveillance capabilities as well. These radars perform critical missions for air traffic control and national security. Although their designs vary, they tend to be similar in some vital receiver characteristics such as noise figure. For this study, NTIA engineers worked closely with personnel from other US Government agencies<sup>16</sup> to determine the susceptibility of two differently designed types of long-range air surveillance radars. Both of these radars operated in the so-called L-band, on individual frequencies assigned between 1250-1350 MHz. In this report these radars are referred to as Long Range Radars 1 and 2.<sup>17</sup>

#### 3.2 Description of Long Range Radar 1

##### 3.2.1 General Description

Long Range Radar 1 detects weather and aircraft within a radius of about 200 nautical miles (370 km) for the FAA and other Federal agencies. It provides data concerning the location and strength of weather as well as range, azimuth, and altitude of aircraft within its search volume. A separate beacon interrogator system that is incorporated into the radar design provides additional information on aircraft beacon codes, aircraft-encoded altitudes, and emergency status<sup>18</sup> of aircraft.

The radar has two channels, denoted as F1 and F2, which require at least 25 MHz of frequency separation.<sup>19</sup> Two frequencies are provided for the purpose of compensating for atmospheric fading, distortion, and other effects on any one frequency; effects that degrade one frequency are not expected to affect the other channel. *Two-frequency capability is not provided for the purpose of using one frequency to compensate for interference effects on the other frequency.* This study did not address radar performance on two channels when one is affected by interference.

Two receiver processing channels, designated A and B and corresponding to each of the two operational frequencies, are provided. Each channel consists of a synchronizer, a frequency generator, a transmitter, weather and target receivers, a receiver processor, and a digital target extractor (DTE). The radar uses frequency separation and orthogonal polarization for the two channels so that they can transmit and receive via the same antenna for the duplex mode of operation. The radar transmits RF energy on a low beam, and receives reflected RF energy on

---

<sup>16</sup> Including the Federal Aviation Administration and the US Air Force.

<sup>17</sup> Long Range Radar 1 is the air route surveillance radar model 3 (ARSR-3), and Long Range Radar 2 is the ARSR-4.

<sup>18</sup> Beacon code, altitude, and emergency status are provided via an associated secondary surveillance radar operating at 1030 MHz and 1090 MHz. Interference to that out-of-band system was not considered in this study.

<sup>19</sup> The tested radar installation operates at 1292.08 and 1330.20 MHz.

both the low beam and a high beam. The high beam is used to detect aircraft at short ranges and the low beam is used to detect aircraft at longer ranges and also weather.

### **3.2.2 Receiver Processing**

Each channel in the radar receiver has both normal and moving target indicator (MTI)<sup>20</sup> video available. The normal and MTI video both have identical constant false alarm rate (CFAR) processing. Both channels contain independent CFAR circuitry. The CFAR samples the input signal at 1/8 mile intervals, from 5/8 mile before the target to 5/8 mile after the target, to determine the mean noise level from the appropriately delayed main target signal.

Long Range Radar 1 also contains integrator-adder circuitry that functions on the normal and MTI video. The integrator-adder contains a digital video integrator. The integrator digitally sums, into a single output, all of the target-hit video occurring within the 1.1-degree (3 dB points) azimuth beamwidth of the radar antenna. Because there are about 12 transmitted pulses within that beamwidth, there can be approximately 12 consecutive target hits or echo returns at the same range and azimuth. Also, since the integrator operates synchronously with the radar's transmitter, asynchronous pulses (from other nearby radars) are automatically eliminated from the video output.

Independent receiver processors in channels A and B are electrically identical. Each receiver processor contains a target processor function. After detection the target information is digitally processed into suitable form for identification by the DTE. When the radar is operating in a two-frequency (called duplex) mode, processed target video data in each radar channel are digitally summed with the adjacent channel target video data before distribution to the DTE. This cross-channel target video summation feature enhances target detection. Cross-channel video summation during dual channel operation improves the probability of target detection since a fluctuating target fade in one channel should not be experienced in the opposite channel due to frequency-polarization diversity between the two channels.

### **3.2.3 Antenna Characteristics**

Long Range Radar 1 uses a dual horn fed parabolic reflector enclosed in a radome and mounted on a dual drive pedestal. The antenna forms two cosecant-squared beams shaped for additional high elevation gain. The two beams are almost identical. The azimuth beamwidth of both beams is 1.1 degrees at the 3 dB points. The upper beam has coverage from 3.6 to 44 degrees in elevation while the lower beam covers 2 to 42 degrees in elevation. The antenna rotates at 5 revolutions per minute (rpm). A complete list of the relevant radar technical parameters is contained in Table 4.

---

<sup>20</sup> Moving target indicator is a Doppler processing output with a velocity threshold. It reduces clutter by eliminating the display of target returns that are moving at less than a critical threshold velocity.



Table 4. Technical Characteristics of Long Range Radar 1

Parameter	Value
Frequency range	1250-1350 MHz
Range	200 nmi
Altitude coverage	Up to 18,300 m (60,000 ft)
Distance resolution	0.25 nmi
Azimuth resolution	2 degrees
Receiver IF bandwidth	420 kHz
Pulse width	2 $\mu$ s
Noise figure	2 dB
Pulse repetition frequency	310 – 364 (8 discrete prf values)
Receiver noise (calculated) level in receiver bandwidth	-115 dBm
Sensitivity with normal processing	-115 dBm
Sensitivity with moving target indicator	-112 dBm
False alarm rate	$10^{-4}$ for a 2-m <sup>2</sup> cross section
Antenna type	Dual horn reflector
Antenna mainbeam gain	Low beam: 34.5 dBi High beam: 33.5 dBi
Antenna elevation beamwidth	cosecant <sup>2</sup> 3.6° to 44° degrees
Antenna azimuth beamwidth	1.1 degrees
Antenna scan rate	5 rpm (12 sec/rev)
Antenna polarization	Linear and circular available

### 3.3 Test Approach for Long Range Radar 1

#### 3.3.1 General

The radar's performance was monitored by observing targets on the radar's PPI display and through the use of the radar's built-in target counting software. Desired targets were generated using RF signal generators and additional testing was accomplished using live traffic. In addition to the desired target signals, signal generators were used to inject CW and binary phase-shift keyed (BPSK) interference into the radar receiver. Radar  $P_d$  performance was evaluated as a function of the calibrated  $I/N$  ratio at the IF output of the radar receiver.

As noted above, the radar could operate on either of channels A and B singly, or on both channels simultaneously. Target power was adjusted to achieve a  $P_d$  value of 0.9 in the absence of interference on a single channel. The same target power was maintained during both single-channel and dual-channel testing on the radar. As a result, the  $P_d$  value was close to 1 when the two channels were used simultaneously. Interference tests were performed in both single-channel and dual-channel operational modes.

### 3.3.2 Injected Targets

In order to speed testing, a total of forty injected test targets (ten targets on each of four separate radials) were separated in range to allow for easy determination of missed targets. They were monitored for five consecutive antenna rotations for a total of 200 injected, desired targets examined for each data point. Each target, regardless of range, was set to the same power at the receiver input, making each target equivalent in terms of receiver  $P_d$ . The target power was adjusted to a level that provided an average target  $P_d$  in the absence of interference of about 90 percent.

The target  $P_d$ , based upon 200 attempted target scans, was based on manual counting from the radar PPI display by one of the authors (Sanders). Although information about target  $P_d$  on a per-pulse basis was collected by the radar's internal data collection software, that information was not used in this study because the radar's overall performance in the presence of interference was the topic of study. (Any one target or "blip" on the radar screen also has an intrinsic  $P_d$  for each individual pulse within the group of pulses that defines that target.) The target generator produced about 12-13 pulses per target. Whenever the radar integrated enough of those pulses to define a target and produce a "blip" on the display, it was counted as a good target. As a result, the actual  $P_d$  per pulse in the group of pulses that defines the target could have been lower than 90 percent.

In order to determine the equivalent radar cross section (RCS) represented by injected test targets, a measurement was made at the end of the test cable connecting the signal generator and the waveguide. Accounting for the waveguide coupler and other losses between the injection point and the receiver, the target signal level into the receiver IF was -107.2dBm.

The radar requirement<sup>21</sup> is for detection at main beam gain of a 2 m<sup>2</sup> target out to at least 195 nmi. One form of the basic radar equation (Eq. 1) is:

$$R = 0.282 \cdot \left[ \frac{P_t G_t A_e \sigma_0}{P_r} \right]^{1/4} \quad (14)$$

where:

- $P_t$  = peak transmit power, watts;
- $G_t$  = transmitter low beam gain, linear term;
- $\sigma_0$  = test target cross section, m<sup>2</sup>;
- $A_e$  = effective antenna aperture, m<sup>2</sup>;
- $P_r$  = received target signal level, watts;
- $R$  = target range, m.

In addition, the Long Range Radar 1 specification allows for a total of 4.1 dB loss in the receiver-to-antenna path. This same loss is also present on the transmitter-to-antenna signal path. For the tested configuration, then:

---

<sup>21</sup> FAA-E-2483b, paragraph 3.4, of the radar System Performance Requirements document.

$$\begin{aligned}
P_t &= 5 \text{ MW} - 4.1 \text{ dB loss} = 1.945 \times 10^6 \text{ W}; \\
G_t &= \text{alog}(34.5 \text{ dB}/10) = 2818.38; \\
A_e &= G_t \lambda^2 / 4\pi = 12.07; \\
P_r &= -107.2 \text{ dBm} + 4.1 \text{ dB} = -103.1 \text{ dBm} = 4.898 \times 10^{-14} \text{ W}; \\
R &= 195 \text{ nmi} = 361235 \text{ m}.
\end{aligned}$$

Rearranging the equation to solve for the test target cross section for a received power of -107.2 dBm, (Eq. 14) becomes:

$$\sigma_0 = \left( \frac{R}{0.282} \right)^4 \cdot \left( \frac{P_r}{P_t G_t A_e} \right) \quad (15)$$

$$\sigma_0 = (361235/0.282)^4 / [(1.945 \times 10^6)(2818.38)(12.07)/(4.898 \times 10^{-14})]$$

$$\sigma_0 = 1.99 \text{ m}^2.$$

### 3.3.3 Live Targets

A limited amount of data were also collected using live ‘targets of opportunity,’ For that testing, the radar was placed into its normal operational mode and the PPI screen was monitored for detected aircraft in the radar coverage area. Though the level of these targets was uncontrolled (being dependent on the interaction geometry between the radar and the aircraft itself), the local FAA air traffic control center was contacted to determine the aircraft type for specific targets of interest on the PPI display.

## 3.4 Undesired Signals in Long Range Radar 1

### 3.4.1 General

RF signal generators and arbitrary waveform generators (AWGs) were used to generate CW interference and also the following BPSK signals:

- 1) BPSK at 0.511 MBit/s,
- 2) BPSK at 1.023 MBit/s,
- 3) BPSK at 5.11 MBit/s,
- 4) BPSK at 10.23 MBit/s.

Spectra of the injected signals are shown in Appendix B. BPSK signals contain data bits that are encoded into symbols that a spreading pseudorandom code further breaks into chips. However, the radar receiver does not discriminate between phase changes representing either a chip or a bit for this type of interfering waveform. The radar receiver processes the BPSK signals as band-limited constant amplitude noise sources, which fall into all of the range cells. Since the noise-like BPSK signal falls into all of the range bins, the CFAR processing cannot eliminate it and the CFAR raises the target detection threshold.

The emission spectrum for each BPSK interference signal was measured and recorded, and tuned to the frequency of the radar channel(s) under test. The BPSK signal generator had the capability to generate  $I/N$  ratios of -12 dB to +30 dB at the receiver RF input; however testing was usually accomplished only over the subset of that range where meaningful  $P_d$  data could be collected. For each signal type, calibrations were performed to allow for conversion between signal generator settings and the resultant  $I/N$  level using the process described in Appendix C.

### 3.4.2 Duration of Interference Signals with Injected Targets

For the injected desired signal tests, the undesired signals were also injected into the radar at the RF input path to the receiver with durations equal to the main beam dwell time and overlaying them on the desired targets at the same azimuth. As shown below, the dwell time for the main beam of the radar's antenna is 0.04 seconds through a stationary object. This dwell time was used as the duration of the BPSK interference source for the simulated target tests. For any live target, this interval may be different due to the motion of the target.

$$dwell\_time = \frac{antenna\_beamwidth}{360deg} \cdot 12sec = 0.04sec. \quad (16)$$

### 3.4.3 Live Target Tests

For the live target tests, as for the injected target tests, the undesired signals were injected into the radar at the RF input path to the receiver (see Figure 10). Because of the mobile characteristics of the live targets however, the injected targets maintained their positions for longer intervals. In particular, the injected targets were controlled so as to cover approximately a 40-degree sector of the radar scan. In addition, for a given set of live targets only a single level of  $I/N$  could be tested. These tests did not attempt to simulate a potential interference source's exact behavior as it might move through the radar's antenna beam at any particular azimuth. The actual dwell time of such an event (and its possible periodicity) would depend upon both the proper motion of the source and the characteristics of the radar antenna beam scanning through space.

## 3.5 Test Procedures on Long Range Radar 1

### 3.5.1 Injected Target Tests

For the injected target tests, the desired signal targets were overlaid with BPSK interference signal at a given  $I/N$  and observed for 5 complete scans. This resulted in a total of 200 possible targets (5 scans x 10 targets/radial x 4 radials/scan), and probability of detection was calculated as the number of observed targets divided by 200. The test was then repeated at a different  $I/N$  level. For these tests the transmitter was turned off and though the antenna was still rotating and receiving external signals, a spectrum analyzer measurement showed that none were present in the IF stage (see Figure 10). When testing was completed for a given BPSK signal type, a different BPSK interference modulation was used and the testing was repeated. For each  $I/N$  level and BPSK modulation, testing was performed with:

- interference and targets on one channel and the other channel disabled;
- interference and targets on both channels;
- baseline “no interference” measurements were performed before and after each “interference” data set.

### 3.5.2 Live Target Tests

For these tests, since the target amplitude was largely uncontrolled, the procedure followed was to operate the radar without injected interference for 15 scans, then turn on the injected BPSK interference at a fixed  $I/N$  for 15 scans, and finally turn off the injected interference for another 15 scans. This allowed for examination of live targets within the BPSK-interfered sector to determine whether there was any discernable impact to the target due to the BPSK interference. The targets were recorded from the PPI display to a radar data file for all 45 scans. Upon replay of the data file to a laptop computer, it was observed that the BPSK interference manifested itself as a reduction of a ‘reinforced target’ (i.e., a primary, skin-track target that had a secondary surveillance radar (SSR) beacon reply superimposed upon it). The skin track part of the reinforced target would fade, but the SSR part, which operates at 1030 MHz/1090 MHz, was not affected.

For targets of interest where a skin-track was lost but the beacon reply was still present, the type of aircraft that was being tracked was determined by contacting the local FAA air traffic control center (ATC) in Kansas City and providing them with the associated beacon code. The ATC was then able to use the beacon code to provide the flight number and type of aircraft to the authors.

## 3.6 Results from Interference Tests on Long Range Radar 1

### 3.6.1 Injected Targets with Single Channel Operation

A plot of the target  $P_d$  versus the  $I/N$  ratio for the radar operating in single channel mode with injected targets and BPSK interference is shown in Figure 19. The figure shows that as the  $I/N$  ratio increases, the target  $P_d$  decreases. At an  $I/N$  level of -9 dB the  $P_d$  curves are beginning to drop perceptibly. At -6 dB  $I/N$  the target  $P_d$  has dropped substantially below the baseline value of 0.9. Detection probability of simulated radar targets (of the minimal acceptable cross section) for single channel operation was degraded by about 0.15 (from 0.90 to 0.75) at the  $I/N$  level of -6 dB.

### 3.6.2 Injected Targets with Dual Channel Operation

A plot of the target  $P_d$  versus the  $I/N$  ratio for the radar operating in dual channel mode with injected targets and BPSK interference on both channels is shown in Figure 20. The figure shows that as the  $I/N$  ratio increases, the target  $P_d$  drops. Figure 20 shows that though the baseline target  $P_d$  per channel was set to the 90 percent value, the overall baseline target  $P_d$  is reinforced (improved) with dual channel operation. But dual channel operation only makes the radar

perform better to a point; at  $I/N$  levels of -6 dB, the target  $P_d$  has dropped below the baseline value. Detection of simulated radar targets (of the minimal acceptable cross section) for dual channel operation was degraded by about 0.10 (from 0.9 to 0.80) from the improved dual-channel baseline at  $I/N = -6$  dB.

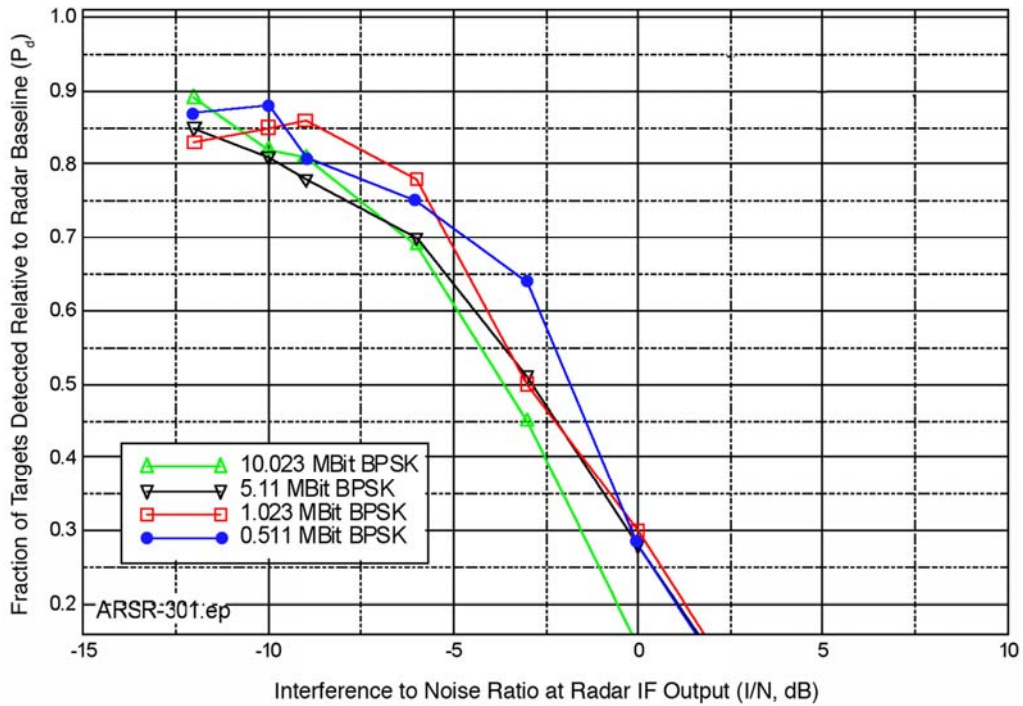


Figure 19. Long Range Radar 1 single channel operation  $P_d$  with BPSK interference.

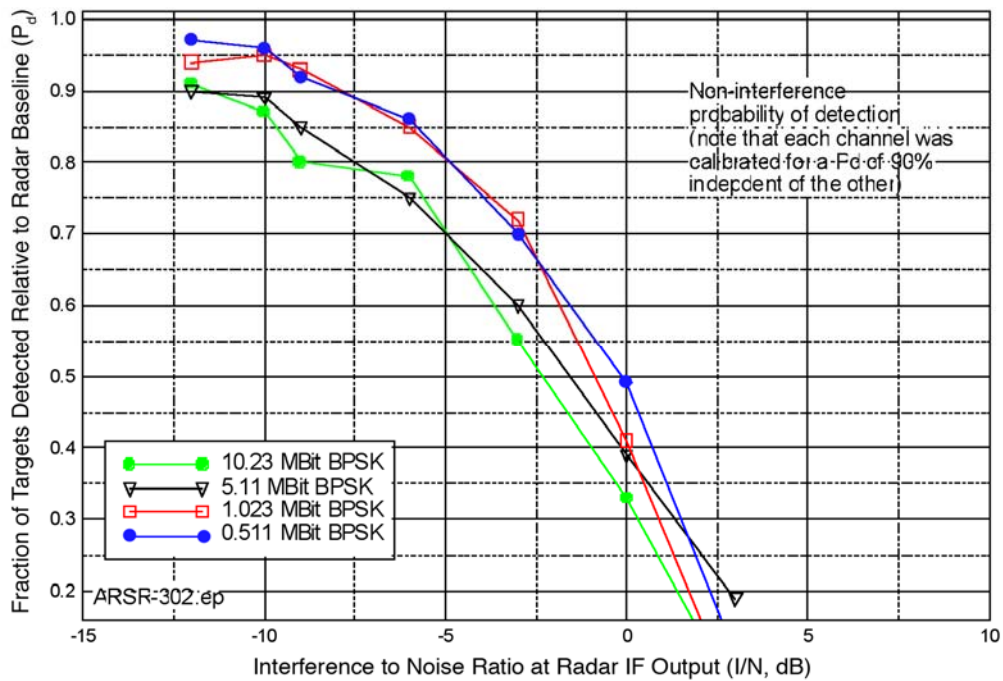


Figure 20. Long Range Radar 1 dual channel operation  $P_d$  with BPSK interference.

### 3.6.3 Results of Live Sky Tests

The 10 MBit/s BPSK waveform was injected into the radar's RF circuitry between the antenna and the receiver (as shown in Figure 10, but with the waveguide connected to the antenna). The  $I/N$  ratio was set to +20 dB for a 40 degree wide azimuth wedge between 160-200 degrees. Figure 21 shows a recording of the aircraft traffic for a full 360 degree view of the PPI display for 45 antenna rotations (scans). Figure 21 represents a 9-minute recording of both skin tracks and beacon tracks from aircraft within the vicinity of the radar. Interference was present during scans 16-30. The figure shows aircraft that were tracked with the radar and beacon. Tracks that are dark represent targets that have both radar track and beacon data. Track segments that are light represent targets with only beacon data.

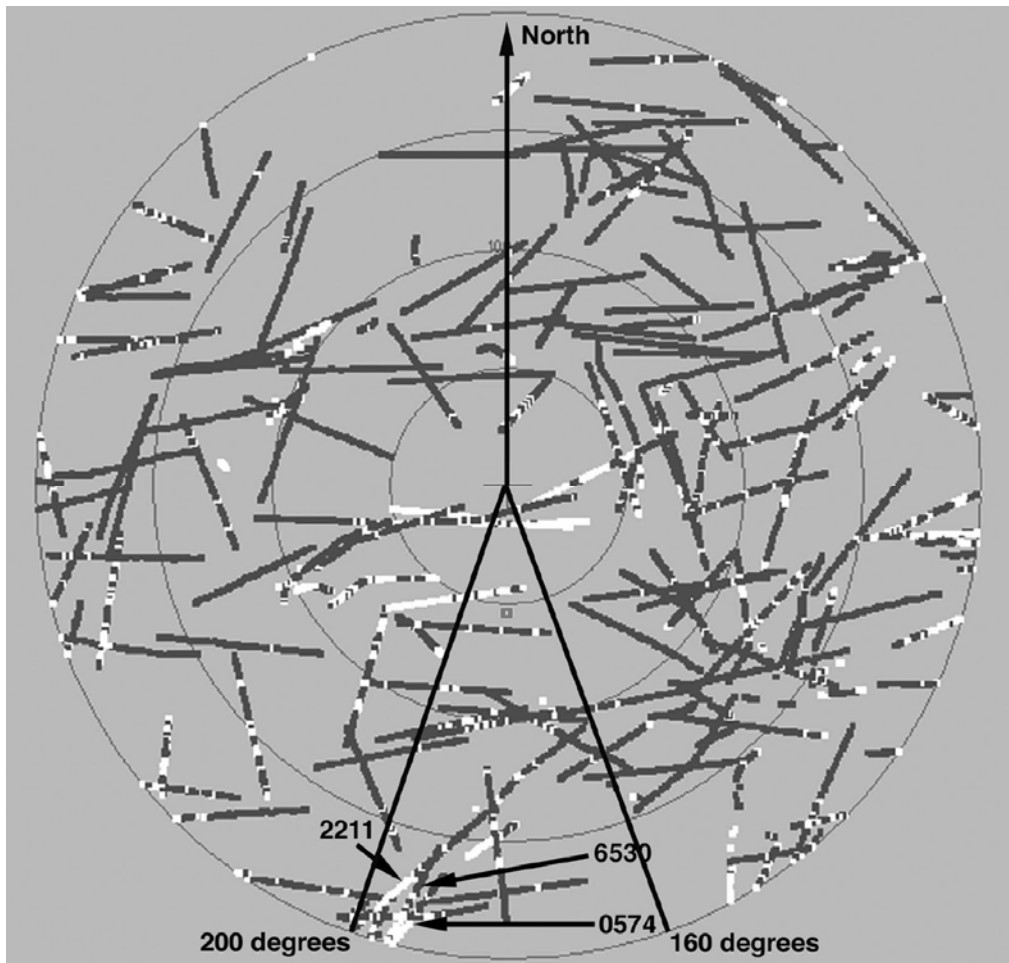


Figure 21. Cumulative PPI display of Long Range Radar 1 for 45 scans during interference in the indicated sector.

Figure 21 shows one aircraft (identified by flight number via the beacon data) within the 160-200 degree wedge of interest that had radar and beacon data for the initial 15 scans (no interference), then only beacon data for the next 15 scans (10 MBit/s BPSK interference), and finally radar and beacon data for the final 15 scans (no interference). The maximum range on the PPI display is 200 nmi. The figure shows that the simulated BPSK interference caused the radar to lose track of this target. The radar also dropped other targets, but the aircraft flew outside of the ATC area before the aircraft type could be identified. Figure 21 also shows that other parts of the PPI output (without known interference) display some aircraft that have intermittent radar data along with their beacon tracks. These are aircraft that may not be fully in the radar's antenna beamwidth due to their altitude and range.

Figure 22 shows the details for the three aircraft of interest. Flight 2211 was an MD-80 observed before, during, and after the interference was injected. The aircraft's initial track is dark, then it goes light, and then it goes dark again. The points where the tracks transitioned from dark represent the circumstance in which interference was turned on. There was a two-scan lag between the moment that interference was switched on or off and the moment at which the resulting effect was observed on the display. Flights 6530 (DC-8 Type 7) and 0574 (TLF-04) entered the interference wedge when the interference was already on. Their tracks begin light (which indicates beacon-only returns being received during interference) and then went dark when the interference was removed (indicating that skin tracking had been restored at that point). The aircraft in question tended to be flying toward or away from the radar station during these episodes. Returns from small aircraft tended to be affected at shorter ranges from the radar than those from larger aircraft, as shown in Figure 22.

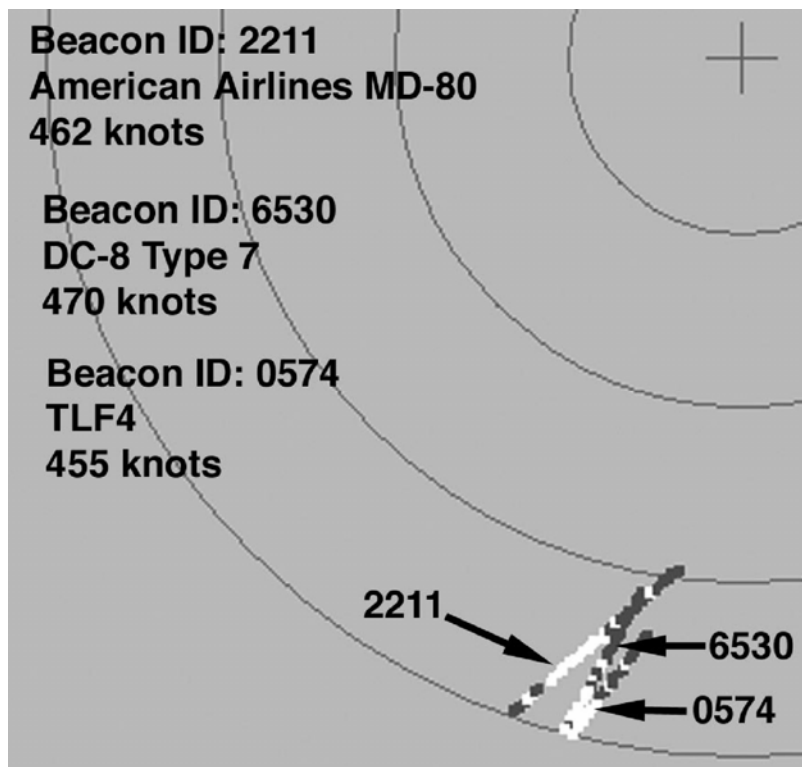


Figure 22. Details of Long Range Radar 1 PPI display during live target interference tests.



### 3.6.4 Test Results from a Second Installation of Long Range Radar 1

Interference tests with injected, desired targets were performed on a second installation of the Long Range Radar 1 model that was at a second location in the U.S. The test protocols were the same as described above, although due to time constraints fewer interference levels were tested on that radar. The results of those tests are shown in Figure 23. Performance was decreased markedly at  $I/N=-6$  dB. The individual channel  $P_d$ 's had been adjusted to 0.9, and therefore the cumulative, dual-channel  $P_d$  values in Figure 23 (which are normalized to the single-channel  $P_d$  values) are higher than 0.9.

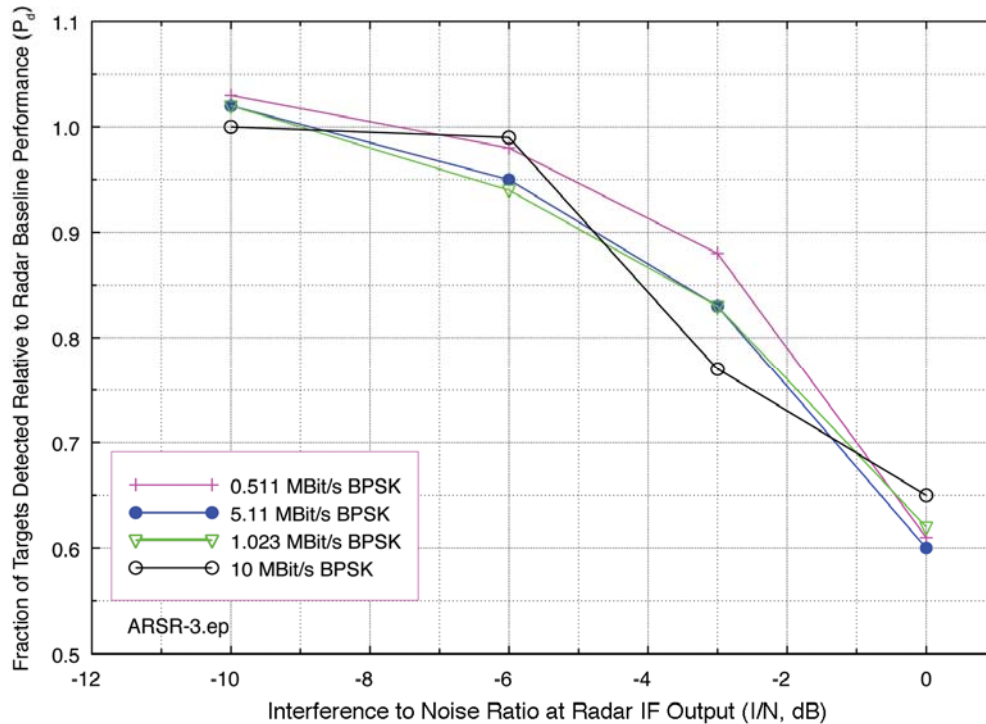


Figure 23. Test results with injected targets at a second installation of the Long Range Radar 1 type.

## 3.7 Description of Long Range Radar 2

### 3.7.1 General Description

Long Range Radar 2 is a coherent, non-linear FM-pulsed system that uses a parabolic reflector, a phased-array feed horn, and all solid-state electronics to meet the needs of both defense and air traffic control. It detects targets at up to 250 nmi (400 km) at an altitude of 100,000 feet. The air traffic control requirement for target detection is  $P_d=0.8$  or more in clear air for a target cross section of  $2.2 \text{ m}^2$  at a range of 200 nmi. To satisfy the defense requirement, the radar was designed for very high reliability (e.g., designed for 1500 hours of mean time between critical failures that would interrupt service) and high sensitivity (including the capability to detect  $0.1 \text{ m}^2$  targets at a distance of 92 nmi against a Sea State 5 clutter-background). The solid-state transmitter power amplifiers are located below the antenna rotary joint to minimize out-of-

service time for maintenance, as the amplifiers can be maintained without halting antenna rotation. The designs of the antenna, the transmitter, and the receiver signal processing hardware and software have all been integrated to optimize the radar’s functionality for both defence and air traffic control requirements. A separate beacon interrogator system that is incorporated into the radar design provides additional information on aircraft beacon codes, aircraft-encoded altitudes, and emergency status of aircraft. General characteristics are summarized in Table 5.

The radar is normally operated in a diplexed (two RF channels) mode, denoted as F1 and F2. Unlike Long Range Radar 1, this radar’s CFAR is *not* independent between the two channels. Two frequencies are provided for the purpose of compensating for atmospheric fading, distortion, and other effects on any one frequency; effects that degrade one frequency are not expected to affect the other channel. *Two-frequency capability is not provided for the purpose of using one frequency to compensate for interference effects on the other frequency.*

Table 5. Technical Characteristics of Long Range Radar 2

Parameter	Value
Tuning range	1215-1400 MHz
Channelization	44 frequency pairs
Uncompressed pulse widths	88.8 $\mu$ s and 58.8 $\mu$ s
Pulse repetition rates	291.5 or 312.5 pps
Pulse modulation	Non-linear FM
3 dB RF bandwidth	58 MHz
3 dB IF bandwidth	690 kHz
Noise figure	3.6 dB
Receiver noise power (in 690 kHz bandwidth)	-112 dBm
Antenna type	Parabolic reflector with phased array feed array
Polarizations available	Vertical, horizontal, RHCP, LHCP
Horizontal scan rate (scan interval)	5 rpm (12 sec/revolution)
Mainbeam gain	41.8 dBi
Beam number one 3-dB beamwidth	Vertical 2.0 degrees, horizontal 1.4 degrees

### 3.7.2 Receiver Processing

Low-noise amplifiers (LNAs) for the RF front-end are located on the flat, phased-array feed array of the antenna. LNAs are installed for row assemblies in the array. LNA outputs are fed from the phased array to the receiver via the antenna rotary joint.

Two receiver processing channels, designated A and B and corresponding to each of the two operational frequencies F1 and F2, are provided. Each channel has a receiver processor and a modular DTE. A built-in tracker can process 800 aircraft plus 200 non-aircraft reports per scan. The radar uses frequency separation and orthogonal polarization for the two channels so that they can transmit and receive via the same antenna in the diplex mode of operation. Figure C-3 shows the radar IF inherent noise spectrum. The receiver’s adaptive threshold algorithm establishes a CFAR level by taking the average signal level over several range bins.

Processed target video data in each radar channel are digitally summed with the adjacent channel target video data before distribution to the DTE. Cross-channel target video summation enhances the probability of target detection since a fluctuating target fade in one channel should not be experienced in the opposite channel due to frequency-polarization diversity between the two channels.

### **3.7.3 Antenna Characteristics**

The antenna is normally located inside a dome and mechanically rotates. The antenna design provides some three-dimensional search capabilities using nine vertically stacked beams that operate up to 30 degrees above the horizon. (The total range of elevation coverage is -7 to +30 degrees.) To obtain accurate data for targets at long range (which will occur at low elevation angles) the low beams are narrower in the vertical dimension than the higher-elevation beams. An interleaving arrangement enables the upper stack of vertical beams to receive nearby target echoes during the inter-pulse intervals of more widely spaced pulses from the lower-elevation beams.

The phased array antenna feed has a flat configuration, is located at the base level of the reflector, and contains approximately 600 radiators that can operate with either linear or circular polarization. Linear polarization is normally used, but circular polarization provides better penetration in rain conditions. As azimuth scans advance, the radar automatically selects the optimum polarization for each of 32 azimuth sectors, depending upon whether each sector contains rain. A significant feature of the radar is side lobes with low gain, which help to reduce clutter and jamming effects.

## **3.8 Test Approach for Long Range Radar 2**

### **3.8.1 General**

The radar's performance was monitored primarily using the built-in target generation and target counting software. Desired signal targets were generated using a built-in, diagnostic RF signal generator. In addition to the desired targets, signal generators were used to inject interference into the radar receive path. The interference was coupled into the radar's RF front end Beam 2 coupler via a fitting that was below the rotary joint. The interference energy and the target energy were both fed through the rotary joint to a built-in coupler on the phased array feed, so that both the desired targets and the interference entered the radar system *ahead* of one of the antenna assembly RF front-end LNAs. Radar  $P_d$  performance was evaluated as a function of the calibrated  $I/N$  level at the IF output of the radar receiver.

### **3.8.2 Injected Targets**

Because the built-in target generator was used to create desired targets for Long Range Radar 2, the test team performed extensive observations of the desired targets to thoroughly understand them and demonstrate their adequacy for the tests. The radar target generator produced simulated

echo pulses that matched the time characteristics of the radar's stagger<sup>22</sup> pattern and, to some extent, the antenna radiation pattern. Figure 24 shows a time-domain scan in the radar receiver IF stage of the pulses comprising a target. The varying amplitudes of successive pulses are a replication of the radar antenna beam shape, and the pulse intervals have the stagger sequence of the radar.

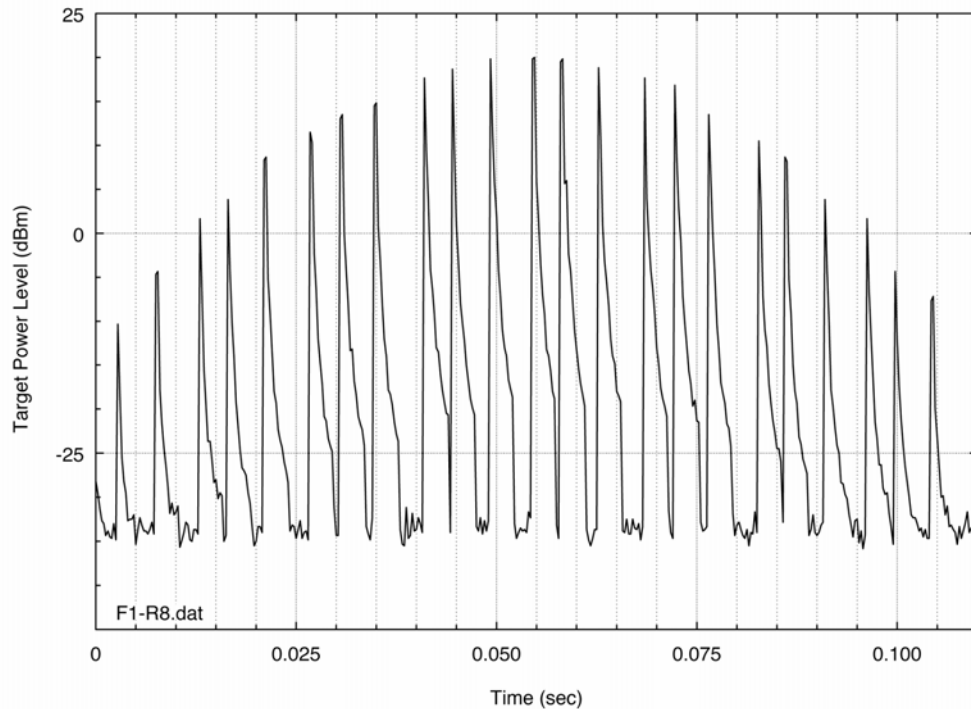


Figure 24. Sequence of desired-target pulses in the IF stage of Long Range Radar 2.

In order to speed testing, a total of 202 injected test targets (distributed in sector wedges on the PPI display) were monitored for 17 consecutive antenna rotations for a total of 3434 injected, desired targets examined for each data point. Each target, regardless of displayed range, was set to the same power at the receiver input, making each target equivalent in terms of receiver  $P_d$ . The target power was adjusted to a level that provided an average target  $P_d$  in the absence of interference of about 90 percent.

The target  $P_d$ , based upon 3434 attempted target scans, was based on automated counting by radar validation software. Whenever the radar integrated enough target pulses to validate a target, it was counted. As was the case for Long Range Radar 1, the actual  $P_d$  per pulse in the group of pulses that defined each target would have been lower than 90 percent.

<sup>22</sup> Stagger is a non-constant pulse repetition interval. It eliminates Doppler-processing 'blind-speeds' that occur at the pulse repetition frequency of fixed-pulse interval radars.

## 3.9 Undesired Signals in Long Range Radar 2

### 3.9.1 General

RF signal generators and AWGs were used to simulate the following interference signals in Long Range Radar 2:

- 1) BPSK at 0.511 MBit/s,
- 2) BPSK at 1.023 MBit/s,
- 3) BPSK at 5.11 MBit/s,
- 4) BPSK at 10.23 MBit/s,
- 5) Carrier wave (CW),
- 6) QPSK at 2 MBit/sec,
- 7) Ultrawideband (UWB) pulses at 10 MHz prf (dithered pulse sequence),
- 8) UWB pulses at 10 MHz prf (undithered pulse sequence),
- 9) BPSK 10 MHz, radiated from a remotely located transmitter.

Spectra of the injected signals are very similar to those shown in Appendix B; with the exception of the CW interference, the interference spectra are lobed ( $\text{sinc}^2$ ) forms. BPSK and QPSK signals contain data bits that are encoded into symbols that a spreading pseudorandom code further breaks into chips. However, the radar receiver does not discriminate between phase changes representing either a chip or a bit for these types of interfering waveforms. The radar receiver will process the BPSK, QPSK, and UWB signals as band-limited constant amplitude noise sources, which fall into all of the range cells. Since the noise-like BPSK and QPSK signals fall into all of the range bins, the CFAR processing cannot eliminate them and the CFAR raises the target detection threshold.

UWB signals consisted of pulsed emissions of  $10^7$  pulses per second at a pulse width of 0.511 ns. The BPSK signal was radiated from the van through an external antenna mounted on a mast towards the radar.

The emission spectra for the interference signals were measured and recorded, and tuned to the frequency of the radar channel(s) under test. (The tuned frequencies for Long Range Radar 2 were 1228 MHz and 1311 MHz.) The loss between the interference signal injection point and the LNA input on the radar feed array was about 74 dB (depending upon the exact path that was used), so that a signal level of about -38 dBm from the interference generator produced about 0 dB  $I/N$  in the radar receiver. The interference signal simulator had the capability to generate  $I/N$  ratios of up to +30 dB at the receiver RF input, but testing was usually accomplished only over the subset of that range where meaningful  $P_d$  data could be collected. For each signal type, calibrations were performed to allow for conversion between signal generator settings and the resultant  $I/N$  level using the process described in Appendix C.

### 3.9.2 Duration of Interference Signals with Injected Targets

Because the injected targets were produced in sector wedges, the interference signals were kept on continuously for about three minutes at a time, which was the duration of each interference

test run at each level for each modulation. To prevent the radar AGC from responding, its value was frozen (at about 80 (arbitrary units)) during the runs. Test results were not affected by the STC state.

Some radiated interference tests were performed with 10 MBit/sec BPSK signals. In these tests, the duration of the interference was only as long as the interval for the radar beam to sweep across the location of a remotely located vehicle that was the interference source, on the order of 0.4 sec per radar scan (Eq. 16). Because the interference was intermittent, AGC was allowed to float for those tests.

### **3.10 Test Procedures on Long Range Radar 2**

#### **3.10.1 Hardline Coupled Interference Testing**

The desired signal targets were overlaid with any one of the interference signals at a given  $I/N$  and observed for 17 complete scans. This resulted in a total of 3434 possible targets (17 scans x 202 targets/scan), and probability of detection was calculated as the number of observed targets divided by 3434. (During UWB interference testing the nominal number of 3434 targets was increased to 4579.)

The interference test runs normally began with a given modulation at a low level (an initial  $I/N$  level of -18 dB or -12 dB). The level was then gradually increased through each run, with 3434 (or 4579 for UWB interference) targets tested at each intermediate  $I/N$  level in increments of about 3 dB, up to  $I/N$  values that sometimes reached +21 dB, but that usually stopped at  $I/N=+5$  or +15 dB. The same interference modulation was always maintained throughout an entire amplitude run. Interference runs were normally performed with:

- interference and targets on one channel and the other channel disabled;
- interference and targets on both channels;
- baseline “no interference” measurements were performed before and after each “interference” data set.

As noted above, AGC was frozen at a fixed level during these runs to prevent adverse effects due to the continuous presence of the interference. This expedient would replicate the behavior of a radar if interference were momentarily encountered in its beam pattern (for about 0.04 sec, as shown in Eq. 16), because in that circumstance the radar would be exposed to interference for such a short period that the AGC would not respond.

The condition of STC (on versus off) was tested to determine whether it would affect the test results. It did not matter, as it turned out, whether STC was activated or not. This was presumably because the targets were displayed at distances that exceeded the STC turn-on interval (which confines the effect to areas that are very close to the radar site).

## 3.11 Results of Tests on Long Range Radar 2

### 3.11.1 Single-Channel Interference Test Results

A plot of the target  $P_d$  versus the  $I/N$  ratio for Long Range Radar 2 operating in single channel mode with injected targets and interference is shown in Figure 25, with a smoothed-curve fit between the data points. The figure shows that as the  $I/N$  ratio increases, the target  $P_d$  decreases. At -6 dB  $I/N$  the target  $P_d$  has dropped several percentage points below the baseline value of 0.95.

### 3.11.2 Dual-Channel Interference Test Results

A plot of the target  $P_d$  versus the  $I/N$  ratio for the radar operating in dual channel mode with injected targets and interference on both channels is shown in Figure 26. The figure shows that as the  $I/N$  ratio increases, the target  $P_d$  drops. The figure shows that although the baseline target  $P_d$  per channel was set to 0.95, the overall baseline target  $P_d$  is reinforced (improved) with dual channel operation to about 0.98. But dual channel operation only helps the radar perform better to a point; at an  $I/N$  level of -6 dB, the target  $P_d$  has dropped several percent.

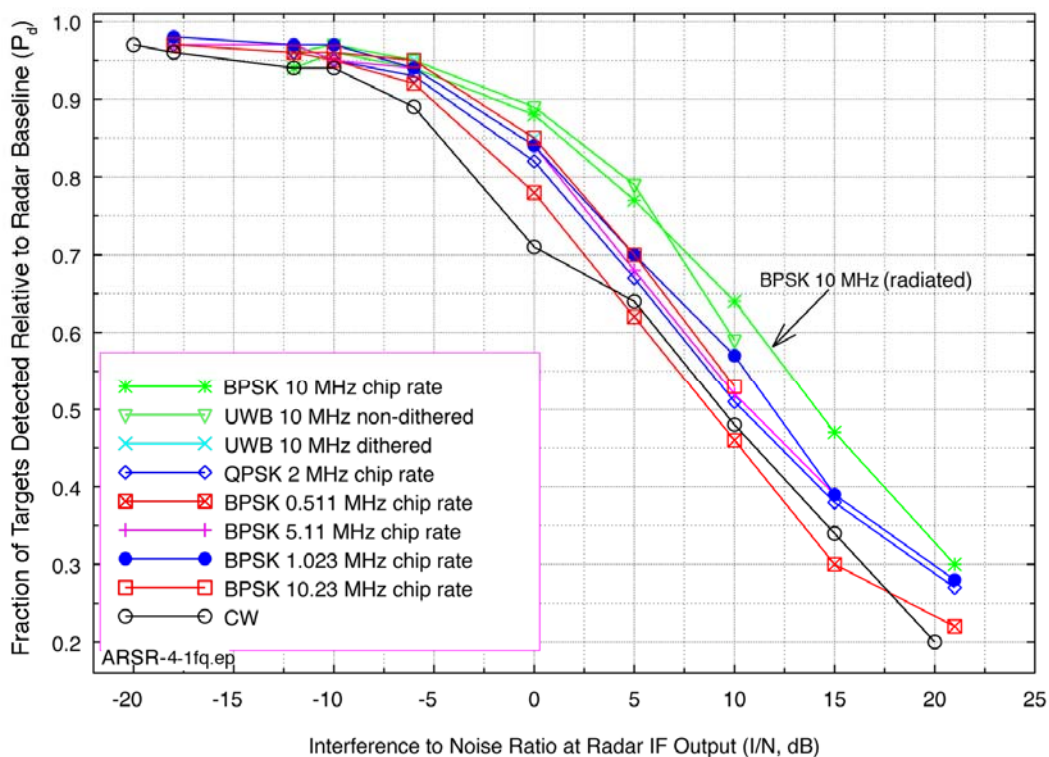


Figure 25. Long Range Radar 2 single channel operation variation in  $P_d$  with interference.

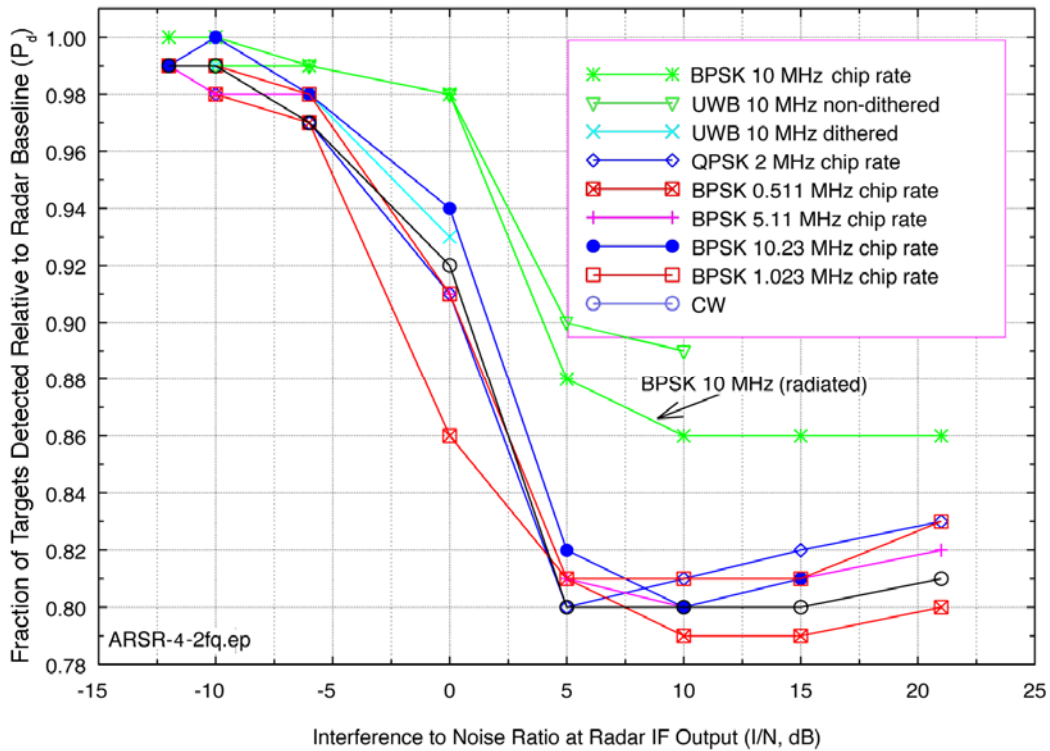


Figure 26. Long Range Radar 2 dual channel operation variation in  $P_d$  with interference.

### 3.12 Summary of Interference Effects on Long Range Radars

From the data obtained, the following general conclusions can be drawn regarding the performance of Long Range Radars in the presence of low-level interference signals:

- The  $P_d$  of simulated radar targets (of the minimal acceptable cross section) for single channel operation showed degradation at interference levels as low as  $I/N = -9$  dB.
- The  $P_d$  of simulated radar targets (of the minimal acceptable cross section) for single channel operation was always measurably degraded, by as much as 0.15 (with  $P_d$  dropping to 0.75 from a nominal 0.90), at  $I/N = -6$  dB.
- The  $P_d$  of simulated radar targets (of the minimal acceptable cross section) for dual channel operation with interference on both channels was degraded by as much as 0.10 (from 0.90 to 0.80) at  $I/N = -6$  dB.
- The beginning of degradation appears to be independent of the interference modulation type. This may be because all modulations that were tested were wider than the radar IF bandwidths. However, this is a realistic condition, in that it is expected that the bandwidth of most interference signals will exceed the bandwidths of most radar receivers.



- Radar dual frequency operation with interference on both channels did not significantly improve performance in the presence of low-level interference, but did seem to keep the  $P_d$  value at 0.8 at  $I/N$  levels of +5 dB and above.
- Live sky tests showed that with an  $I/N$  of +20 dB and a 10 MBit/s BPSK interfering signal, the radar lost track of some targets near the edge of its coverage range.
- While the effects of strong interference in radar receivers can be very dramatic, as shown in Figure 27, *the damaging effects of low-level interference in radar receivers are insidious because there is no overt indication that interference is occurring*, as shown in Figure 28. For low levels of interference (typically less than  $I/N=+3$  dB), target losses were not accompanied by any other indications that interference was occurring. Were such losses to occur during normal radar operations, the operators would probably not be aware that targets that should otherwise have been detected were missing, nor that any interference was occurring. It is suggested that one reason that low-level interference effects are rarely reported by radar operators is the subtle, insidious nature of such interference in radar receivers.
- Loss of desired targets in the presence of interference is purely a function of the target echo level relative to the radar receiver noise limit; target range from the radar is not a factor, as illustrated, for example, in Figure 28. It is true that, all other factors being equal, targets at long ranges will return weaker echoes than closer targets. But all other factors are *never* equal; target cross sections vary. Therefore, *any target at any distance from a radar can be lost due to interference when its return echoes are weak*. This means that *low-level interference will not just result in loss of targets at the edge of radar coverage*. Weak targets that are close to radar sites will be lost as well. Weak targets, at any range, are just as critical in national defense and safety considerations as larger cross section targets at the edge of radar coverage; small cross section targets at short ranges may be *more* critical in some situations.

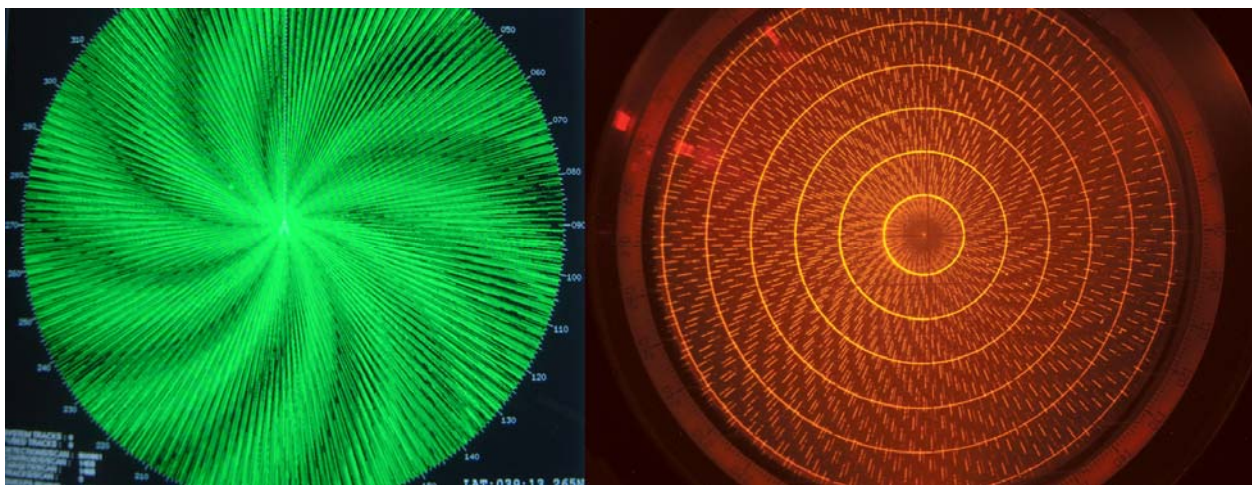


Figure 27. The effects of strong interference in two radar receivers, such as these examples where  $I/N$  is on the order of +20 dB, will normally be obvious to operators. (When such effects occur on single azimuths they are visible as bright lines called strokes.)

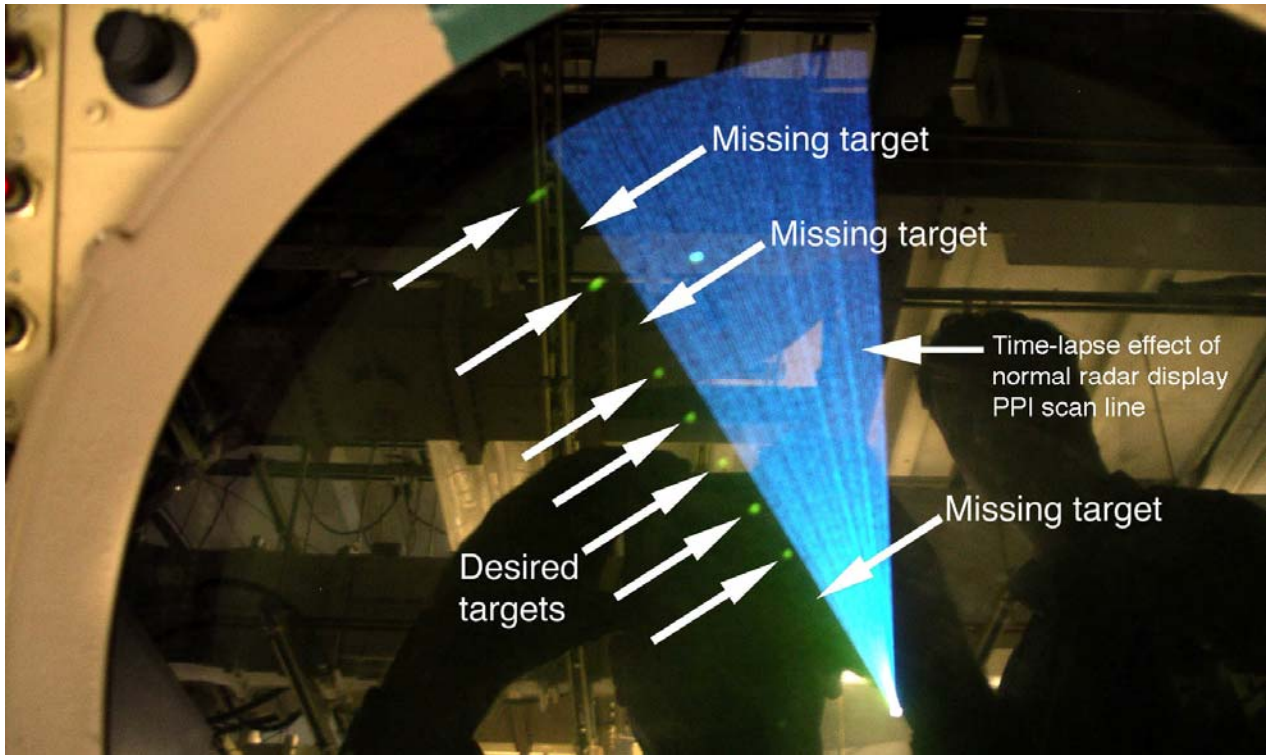


Figure 28. In contrast to the effects of strong interference in Figure 27, target losses due to low-level interference effects (occurring here at an  $I/N$  level of about -3 dB in Long Range Radar 1) are insidious; *there is no indication on the PPI display that interference is occurring*. The insidiousness of the phenomenon of low-level interference in radar receivers is of considerable concern because of its implications for adverse impacts on radar missions without even the possibility of warning indications for operators.

## **4 INTERFERENCE MEASUREMENTS ON A SHORT-RANGE AIR SEARCH RADAR**

### **4.1 Introduction**

Interference measurements and tests were performed to determine the effects of emissions from digital communication signals on a short-range air search (radionavigation) radar operating within the primary allocation for airport surveillance radars (ASRs) in the 2700-2900 MHz band. Such radars are operated at shorter ranges than the radars examined in the previous section, typically on the order of 100 nmi.

The radar that was tested employs pulse widths, prfs, IF bandwidth, noise figure, and antenna beamwidths typical of those identified in an ITU-R Recommendation for radars in this band [20]. Those radars typically employ interference mitigation techniques/processing methods identified in another ITU-R Recommendation [18] to allow them to operate in the presence of other radionavigation and radiolocation radars. As noted in Section 1, those techniques are effective in reducing pulsed interference between radars but not high duty cycle interference from communication signals.

The tests described here investigated the effectiveness of the radar's interference suppression circuitry and software to reduce or eliminate interference due to the emissions from communication signals employing a digital modulation scheme.

#### **4.1.1 Objectives**

The objectives of the testing were to:

- quantify the capability of a short-range air search (radionavigation) radar's interference-rejection processing to mitigate unwanted emissions from digital communication systems as a function of their power level;
- develop  $I/N$  protection criteria for unwanted digital communication systems emissions received by such a radar;
- observe and quantify the effectiveness of the short-range air search radar's interference rejection techniques to reduce the number of false targets, bright radial lines on the PPI display (strokes), and background noise.

### **4.2 Short Range Air Search Radar Technical Characteristics**

#### **4.2.1 General Characteristics**

The short-range air search radar that was tested is used for monitoring air traffic near airports, and is also referred to as a terminal radar. Nominal values for the principal parameters of this radar are presented in Table 6.

Table 6. Technical Characteristics of the Short-Range Air Surveillance Radar

Parameter	Value
Frequency	2700-2900 MHz
Maximum range	60 nmi
Pulse width	1.08 $\mu$ s
Pulse repetition frequency	928 and 1193 Hz; 1027 and 1321 Hz
IF bandwidth	653 kHz
Spurious response rejection	60 dB
System noise figure	4 dB
RF bandwidth	10 MHz
Antenna scan rate (scan time)	12.5 rpm (4.8 sec/revolution)
Antenna horizontal beamwidth	1.4 degrees
Antenna vertical beamwidth	4.8 degrees
Polarization	Right-hand circular or linear

The radar divides its 60-nmi operational range into 1/16-nmi intervals and azimuths, and each of those by 256 intervals of approximately 1.4 degrees each, for a total of 245,760 range-azimuth cells. In each 1.4-degree azimuth interval the transmitter sends ten pulses at a single prf and then sends eight pulses at a lower prf. The receiver processes each set of 18 pulses to form 18 Doppler filters. Alternating prfs within every 1.4-degree wedge helps to eliminate blind speeds, unmask moving targets hidden by weather, eliminates second-time-around clutter returns, and divides the radar output into approximately 4,483,584 range-azimuth-Doppler cells.

#### 4.2.2 Antenna Characteristics

The radar employs a parabolic reflector with two horns, for high and low beams, in the antenna feed array. Target echo pulses received by the high and low beam horns in the antenna array are amplified by RF front-end low noise amplifiers and are sent via toggle-switched paths to their respective receivers. The high-beam horn receives returns from high elevation-angle targets close to the antenna, while the low-beam horn receives returns from low elevation-angle targets at greater distances. The high beam receiver reduces clutter strength at short ranges in order to improve sub-clutter visibility.

For these tests, the low beam receiver was selected because the radar would be most likely to receive interference from local ground-based emitters through this path. The low beam is used for observation of targets at ranges exceeding about 15-20 nmi. The beams are not used simultaneously; the radar receiver toggles sequentially between them. The coverage patterns for the high and low beams for a 1 m<sup>2</sup> target cross section with  $P_d=0.80$  are shown in Figure 29.

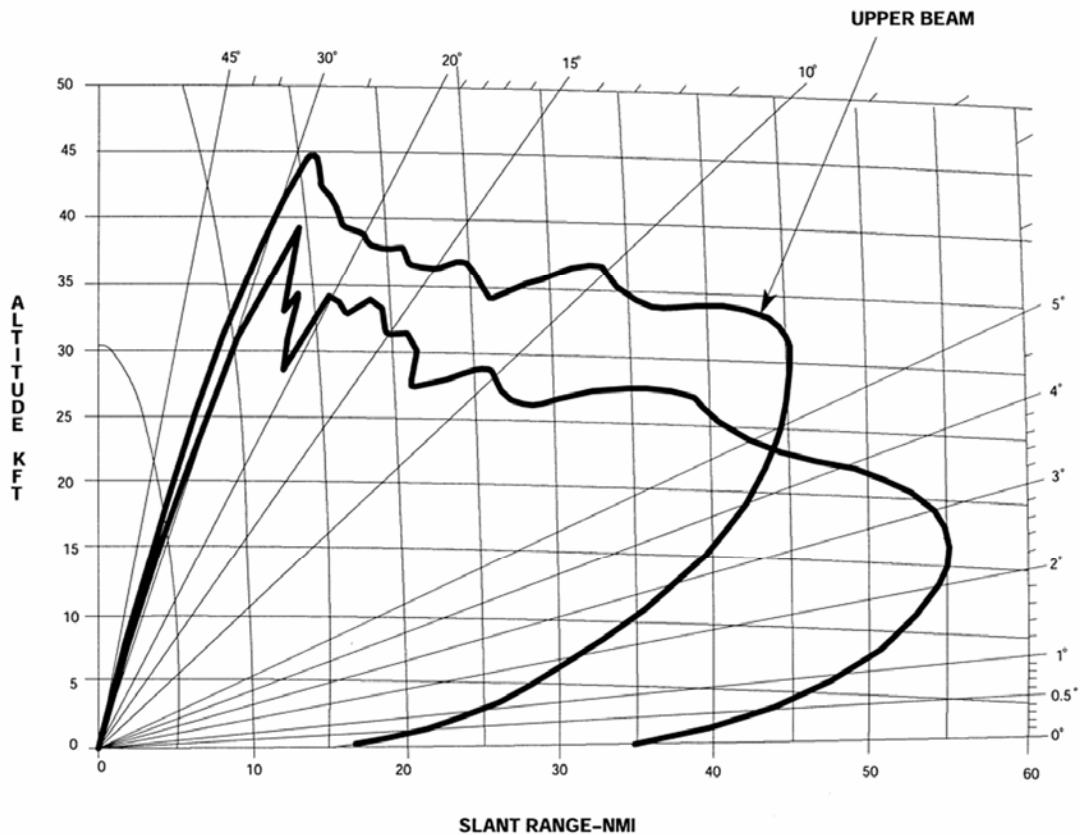


Figure 29. Beam coverage patterns for the short-range air surveillance radar.

### 4.2.3 Target Receiver

The target receiver/processor employs STC and Moving Target Detection (MTD), which includes Doppler filtering and CFAR processing, to detect and separate target returns from noise, ground clutter, and weather. The target receiver/processor sorts the target returns according to range, detects their Doppler shifts, and sends them to the radar system post processor.

### 4.2.4 STC

The radar uses STC in its receiver to provide attenuation immediately after the start of the transmitted pulse to decrease its sensitivity at close range, as described in Section 1 of this report. The radar STC curve is shown in Figure 5. The STC was disabled during the tests, but the target amplitudes were set at values that would not have been affected by STC even if it had been active.

### 4.2.5 IF Circuitry

The IF receiver amplifies the outputs of the RF receiver and detects their phase shifts. The IF circuitry consists of a three-stage logarithmic video detector/amplifier with a wide dynamic range

and I and Q phase detectors. The output of the IF amplifier receiver is at 31.07 MHz. A CW signal swept at RF frequencies was applied as an input stimulus to the radar receiver to obtain the receiver's 3-dB bandwidth, which was measured to be about 680 kHz at the input to the phase detectors. The receiver's response to the swept CW signal is shown in Figure C-4. The dynamic range of the radar receiver was measured by varying the power level of a fixed frequency CW signal and monitoring the output of the IF circuitry at the same test point. Figure 30 shows the gain characteristics of the radar receiver. Measurable compression occurs with an input signal power level of about -43 dBm.

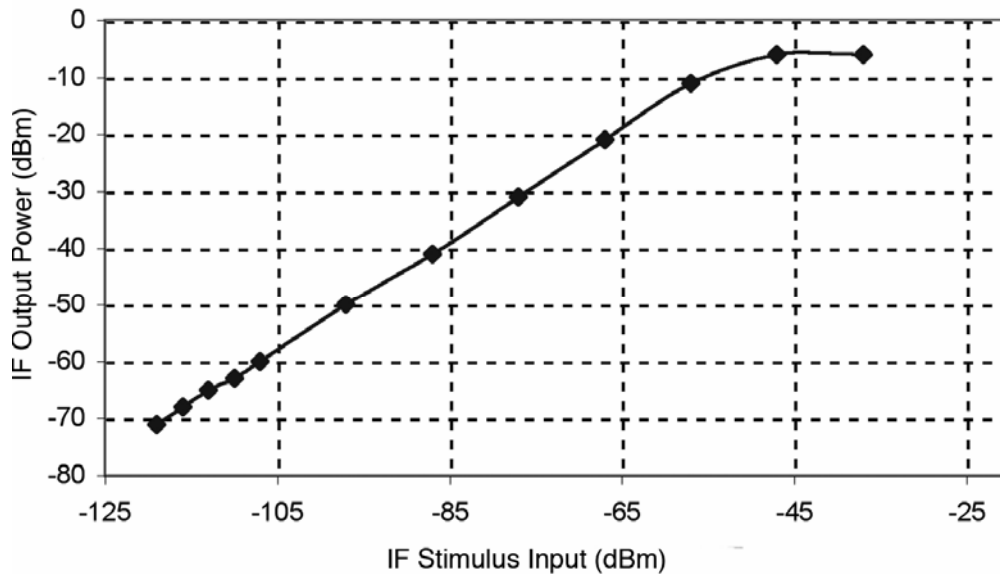


Figure 30. Short-range air surveillance radar input/output gain curve.

The phase detectors at the output of the IF amplifier determine the change in phase between the returns and the transmit pulses that produced them, using the coherent oscillator (COHO) from the frequency generator as a transmit-pulse phase reference. The phase detectors each have sinusoidal responses, and produce in-phase (I) and quadrature (Q) outputs with a sine-cosine (90 degree) phase relationship to each other. Because the I and Q phase detector responses are sine and cosine functions, their outputs can be vector-summed to determine the actual magnitude of the target returns. Software-implemented servo loops set the DC offsets, gain balance, and phase balance of the I and Q outputs based on the state of the phase detectors. They also set the AGC level of the RF and IF amplifiers to limit the noise level within one quantum (the change in RF level represented by the least significant bit (LSB) output of the analog-to-digital (A/D) converter) of the radar internal noise level.

The I and Q outputs of the IF circuitry are sampled and digitized by A/D converters during each 0.77  $\mu$ s (equal to 0.75 percent of the transmitted pulse width), covering a 1/16-nmi range cell, at a clock rate of 2.6-MHz. The results are then interleaved. The A/D converter produces 12-bit digital words that represent the samples of the I and Q signals to the filter and magnitude processor.

#### **4.2.6 Doppler Filtering**

In each 1/16-nmi range cell, coherent processing intervals (CPIs), consisting of returns from alternately 10 and 8 successive pulse repetition intervals, are formed. In the 10-pulse case, the batches associated with each successive 1/16-nmi range increment are sequentially applied to the same set of 10 Doppler filters. The radar random access memory (RAM) stores digital representations of the returns over several pulse-repetition trains (PRTs) and the Doppler filters process them together so that pulse-to-pulse changes in target-return amplitudes (representing apparent Doppler frequencies) can be calculated. For the 10-pulse CPI, five of the filters are used to detect targets moving towards the radar antenna and the other five are used to detect receding targets. A similar process is used for the 8-pulse CPI, except that eight filters are used. The Doppler filters improve the receiver's signal-to-noise ratio because the Doppler filters add or integrate a series of target returns at their frequency. This causes return signals to progressively accumulate at the output of the filter, while random-frequency noise accumulates at the filter outputs at a much slower rate.

#### **4.2.7 CFAR Processing**

The radar uses a 27-cell sliding-window averaging (or range averaging) CFAR technique to calculate the mean level threshold (MLT). (CFAR processing automatically varies a detection threshold to maintain false target declarations, based on the return signal plus noise outputs of the Doppler filters at a constant rate, as described in Section 1 of this report.) Each Doppler filter sums the energy contained in the stream of returns received as the antenna sweeps over a target. The energy combines with the noise energy that accumulates in the filter during the same time interval. If the integrated signal plus noise at the output of a filter exceeds the MLT, the detector concludes that a target is present.

Thresholds for the non-zero velocity resolution cells are established by summing the detected outputs of the signals in the same velocity filter in a 27-cell window centered about the cell of interest. Thus, each filter output is averaged to establish the mean level of non-zero velocity clutter. Filter thresholds are determined by multiplying the mean levels by an appropriate constant to obtain the desired false-alarm probability.

Random noise will occasionally exceed the MLT and the detector will falsely indicate that a target is present. The higher the detection threshold to the mean level of the noise energy the lower the probability of a false alarm will be, and vice versa. If the detection threshold is too high, valid targets may go undetected. The outputs of the Doppler filters are continuously monitored to maintain an optimum threshold setting. The CFAR sets the detection thresholds to maintain the false alarm rate for each Doppler filter at an optimum value. A QPSK-type waveform covering the band of the radar receiver will appear simultaneously in all the Doppler filters as noise and cause the CFAR to raise the detection threshold, causing all targets to have a correspondingly lower probability of detection.

### 4.3 Interference Procedures and Methods for the Short Range Air Search Radar

#### 4.3.1 Interference Signals

Three types of interference signals were injected into the radar as unwanted emissions through a 20 dB coupler port in the receiver's waveguide path, as shown in Figure 31. The signals were an un-modulated continuous wave (CW), a continuous 2-MBit/s QPSK waveform, and a 2-MBit/s QPSK waveform with a 1/8 time slot duty factor. All three signals were co-channel with the radar's operating frequency and occurred within the full 360 degrees of the antenna's rotation. The continuous and pulsed QPSK waveforms represent the type of signals that would be expected to be used by digital communication systems such as IMT-2000 in CDMA and TDMA

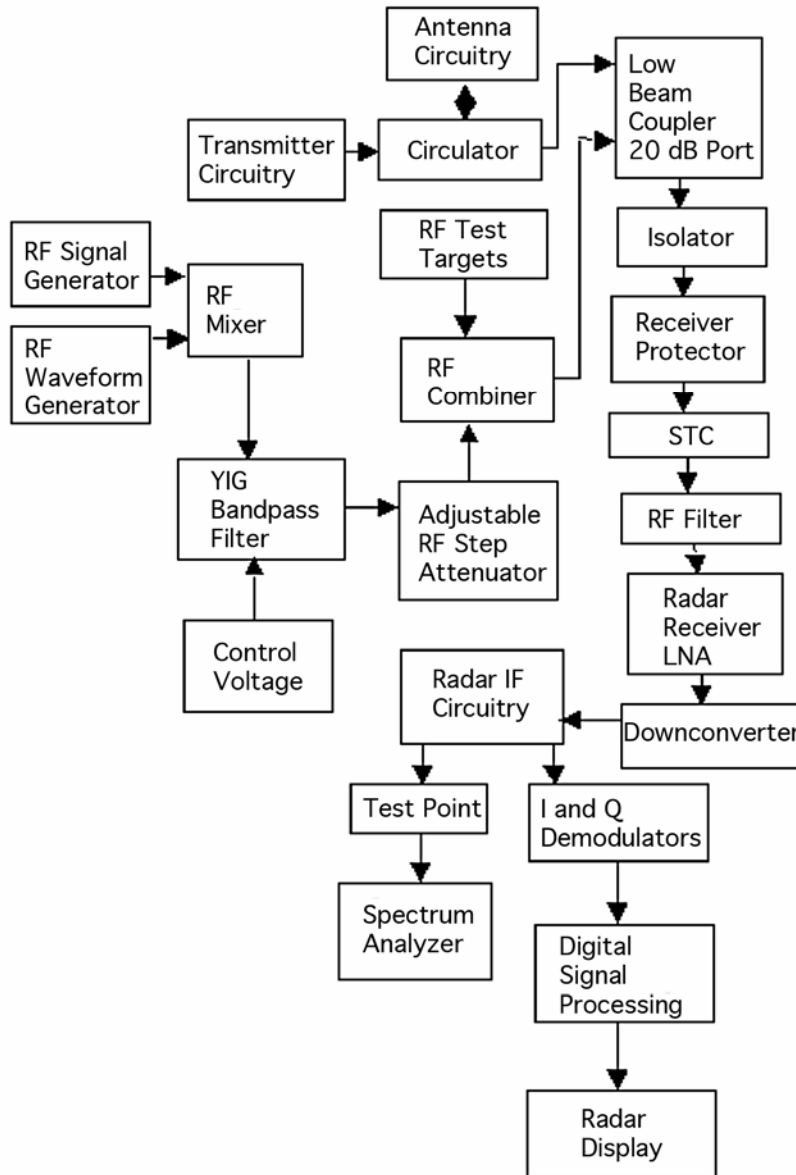


Figure 31. Test set-up for interference injection into short-range air search radar.



systems, respectively. The measured emission spectrum of the continuous QPSK signal is shown in Figure B-5. The QPSK signal was generated and injected into the short-range air search radar using the test set-up shown in Figure 31.

The CW signal was simulated using an RF signal generator. For the CDMA type QPSK waveform, an AWG was programmed to output a QPSK waveform at a data rate of 2 MBit/s. The program simulated a uniform distribution of random bits containing no repetitions with a code length long enough to ensure that no spectral lines occurred within the bandwidth of the radar receiver. For the TDMA (time-sliced) type QPSK waveform, another AWG was used to pulse the QPSK waveform for a 1/8 time slot duty factor. The on-time of the pulses was 577  $\mu$ s and the repetition period was 4.6 ms.

The output of the AWG was fed to a mixer whose other input was connected to an RF signal generator. The RF signal generator functioned as a local oscillator and its frequency was adjusted so that the carrier of the QPSK waveform was co-tuned with the radar receiver. A YIG bandpass filter was used to suppress any spurious emissions that resulted from the mixing process. An RF step attenuator immediately after the YIG filter was used to control the power level of the QPSK emissions.

#### 4.3.2 Target Generation and Counting

Ten simulated, equally-spaced targets were generated along a radial using the radar's built in test target generator (consisting of a combination of hardware and software). The targets on the radial had a constant power envelope. Each target count  $P_d$  was made with 20 rotations of the radar; in 20 rotations, 200 targets were generated. The value of  $P_d$  was determined by dividing the number of counted targets by 200. For example, if 180 targets were counted the  $P_d$  was 0.90. The targets were counted manually, by observing the correlated video output on the radar's PPI display.

#### 4.3.3 Test conditions

The tests were performed with the parameters shown in Table 7 set on the short-range air search radionavigation radar.

Table 7. Control Settings for the Short Range Air Surveillance Radar

Receiver Parameter	Value
Sensitivity time control (STC)	Off
Interference rejection (IR)	On
Automatic gain control (AGC)	On
PPI image selected for target counting	Processed video
Radar range mode	60 nmi

#### 4.3.4 Test Procedures

The RF power output of the target generator system was adjusted so that the target  $P_d$  was as close as possible to 0.90 (given that the target levels could only be adjusted in 1-dB increments) without interference being present (for correlated video targets). As noted above, targets were counted in twenty scans to set the baseline  $P_d$ . The radar was observed to have a sort of memory of target conditions, as the target  $P_d$  was slow to change when the target power level was adjusted using the target control software. Due to the CFAR processing, the radar took 8-10 scans before it would reach a new steady state after the target power was adjusted.

After the radar was set to its baseline condition, the CW and QPSK interference was injected into the radar receiver. The power of the CW and QPSK signals that were injected into the radar receiver was set to different levels while the power level of the targets was held constant.

The power levels of the CW and QPSK signals were set to values that produced  $I/N$  levels of -12 dB, -10 dB, -9 dB, -6 dB, -3 dB, 0 dB, +3 dB, and +6 dB in the IF circuitry of the radar receiver, as described in Appendix C. To account for the radar's target memory, the targets were not counted until 10 scans had occurred after the interference had been enabled. After 20 scans with the interference enabled and the targets counted, the interference was disabled and an additional 10 scans were allowed to occur before the next  $I/N$  level was tested. Waiting 10 scans to occur *between* each change in target and interference conditions ensured that each measurement was not affected by the previous one.

As the CW and QPSK power levels were varied, the display of the radar was observed for any increase in the number of false targets, bright radial streaks or lines (strokes), or any increase in background speckling.

#### 4.4 Test Results for the Short Range Air Search Radar

Curves showing the target  $P_d$  versus the  $I/N$  levels were produced for the CW, CDMA-QPSK, and TDMA-QPSK interference are shown in Figure 32. The data in Figure 32 show that all three emissions caused a reduction in the target  $P_d$  ranging from 9 to 25 percent for  $I/N$  levels equal to -6 dB. The TDMA type emission did not cause as much of a reduction in the target  $P_d$  at the higher  $I/N$  levels as the other waveforms. This is believed to be because the radar's CFAR was able to treat it as pulsed interference and reduce its effects to some degree. However, the radar's operation was still adversely impacted. Furthermore, higher time-slot duty factors would increase the effects from the TDMA waveform, until at some point they would equal the effects from the CDMA type signal.

#### 4.5 Summary of Interference Effects on a Short-Range Air Search Radar

The  $P_d$  interference curves show that the short range air search radar's target detection capability was adversely impacted at an  $I/N$  level of -6 dB. This result is consistent with the observations of the behavior of the long range air search radars.

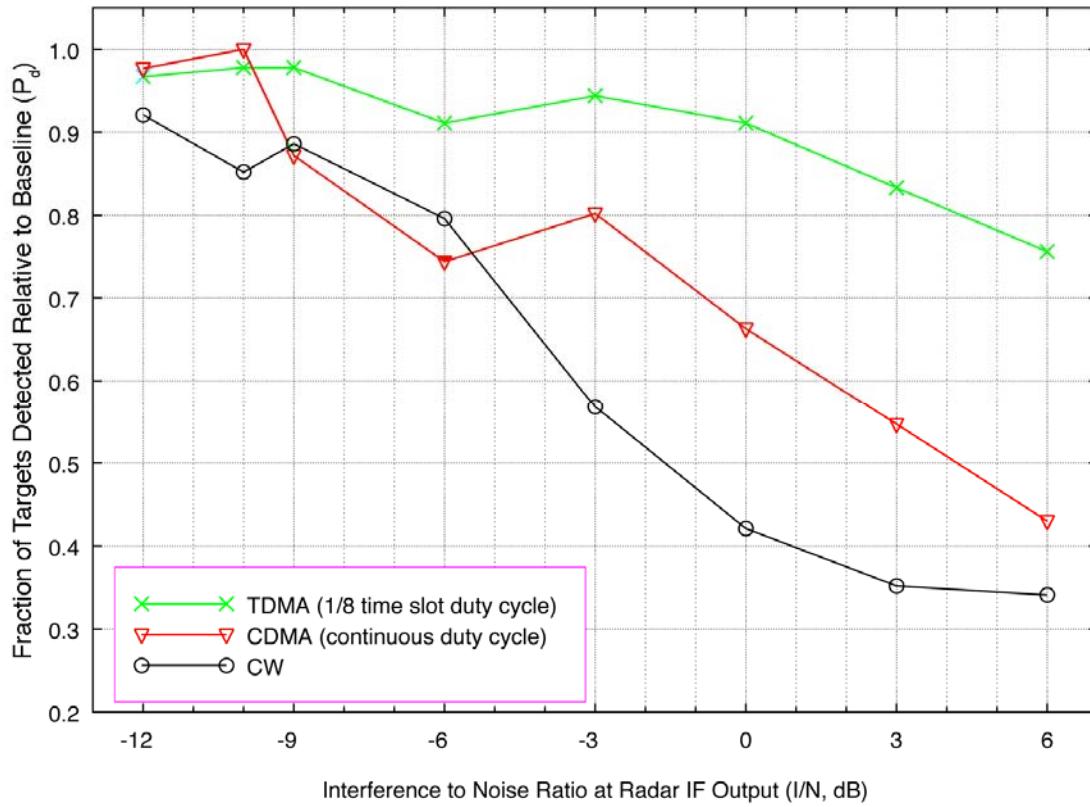


Figure 32. Interference response curves for the short-range air search radar. CDMA-2000 mobile terminal modulation was used for these tests.